Lithosphere, Ionosphere, and magnetosphere couplings : the LIMADOU Project

Vincenzo Vitale on behalf of the PG-TN-ASDC team
(R.Battiston,William Burger, Filippo Ambroglini and V.V.)

- Litho–Iono-Magnetosphere couplings and Earthquake monitoring
- Early measurements of MeV electrons
- Current Studies
- The CSES mission

HILITE Workshop, 29th Sept -1st Oct 2013, Torino

Earthquakes

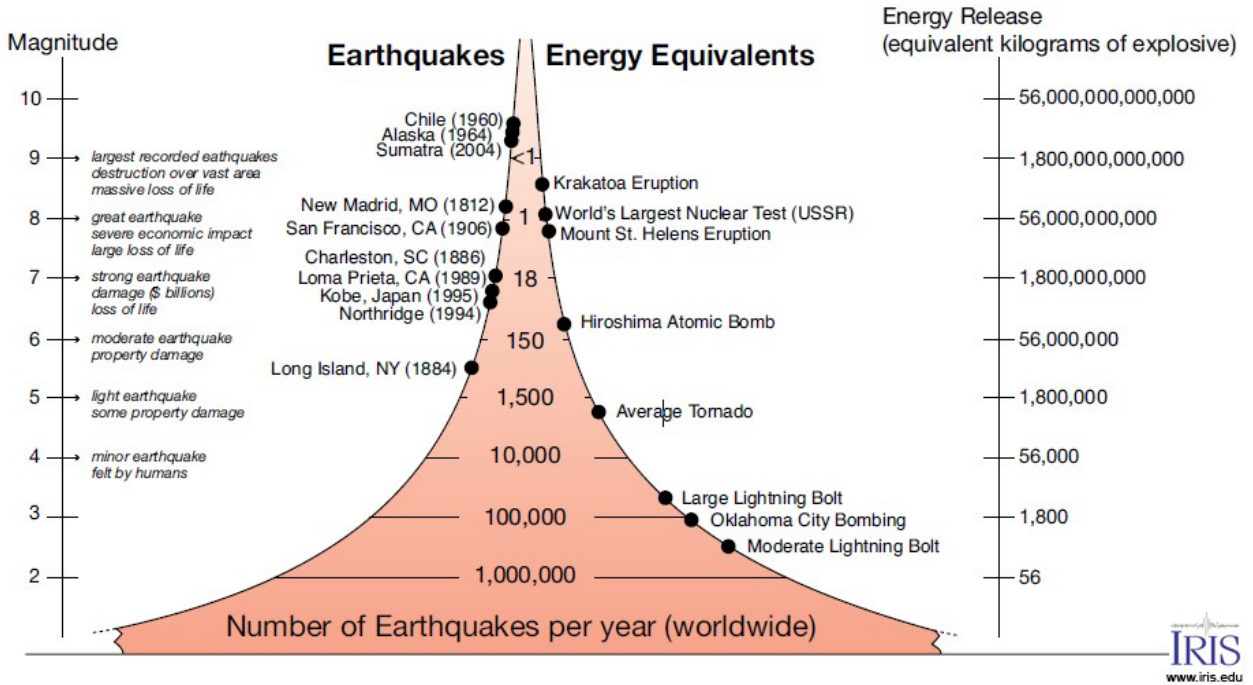

- Very complex phenomenon
- Long preparation phase
- Changes of physical parameters
- Over a large surface
- Large energy release

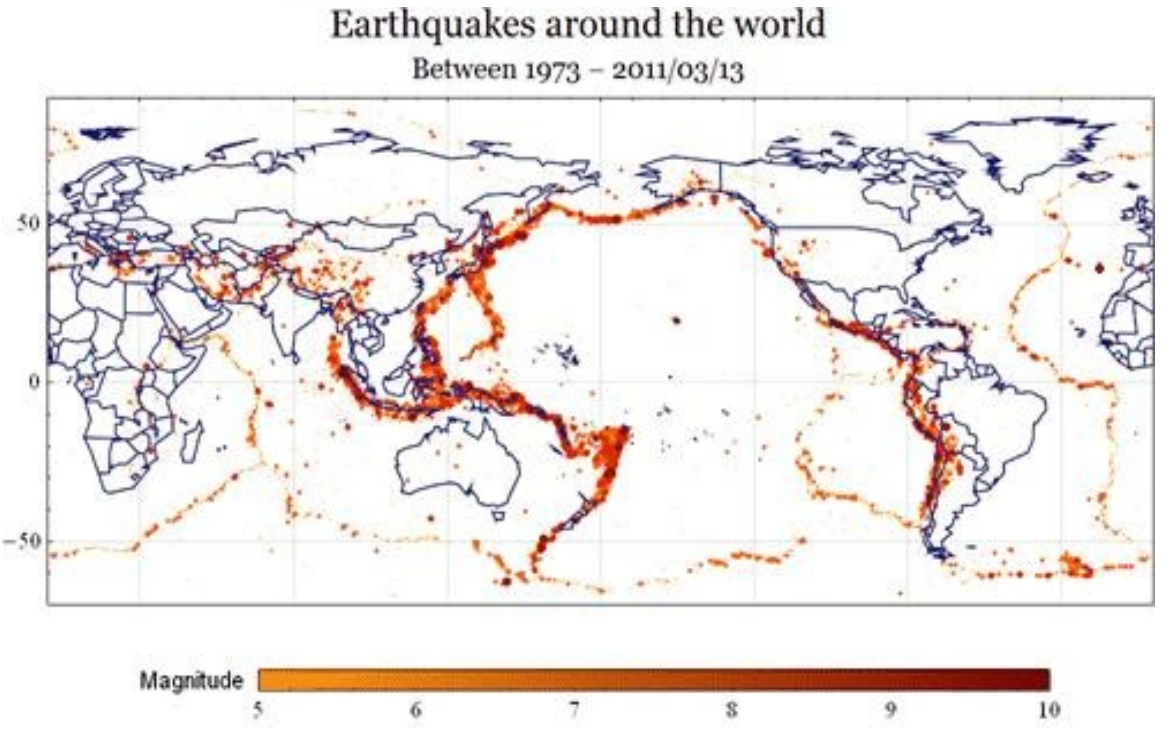

Litho–Iono-Magnetosphere couplings and Earthquake monitoring

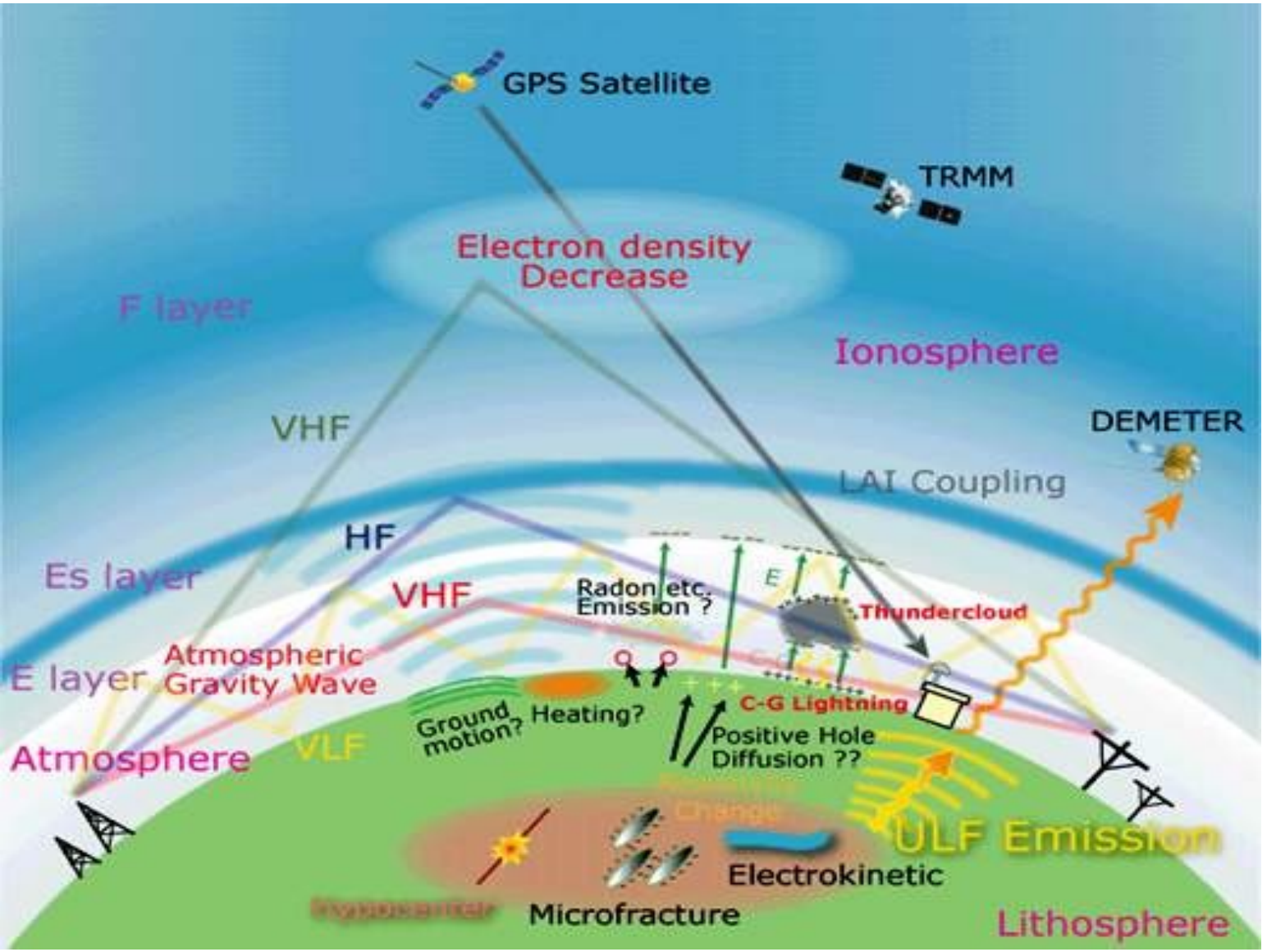

Thermal Infrared Rad. (months)

Total Elect. Content and GPS disturbances (days)

Particle Burst (hours)

How Earthquakes can couple with Ionosphere and Magnetosphere

Litho–Ionosphere coupling: an example

JOURNAL OF GEOPHYSICAL RESEARCH, VOL. 116, A10317, doi:10.1029/2011JA016628, 2011

Ionosphere plasma bubbles and density variations induced by pre-earthquake rock currents and associated surface charges

C. L. Kuo,[1,2] J. D. Huba,[3] G. Joyce,[4] and L. C. Lee

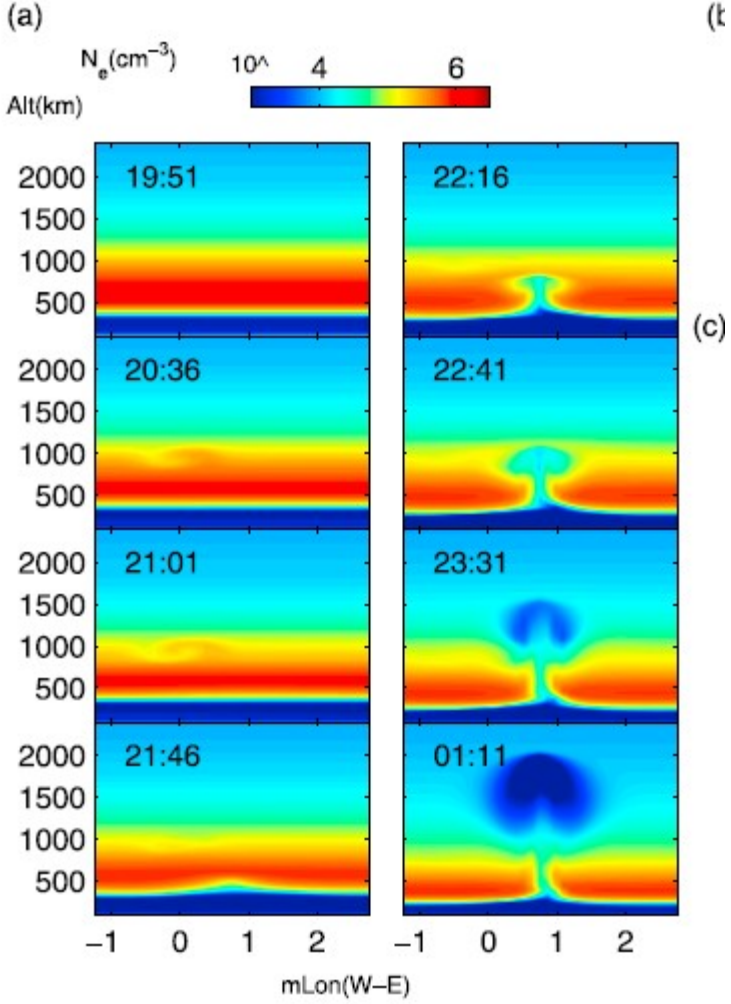

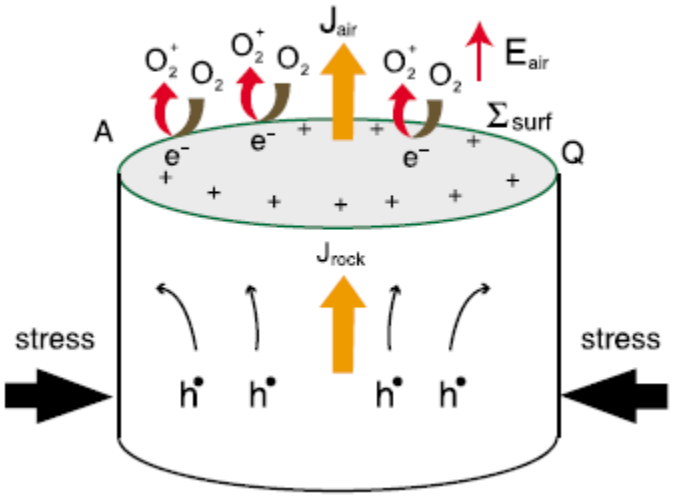

Figure 7. (a) Contour plots of electron density N_e in the equatorial plane at different times for the nighttime case with current density $J_{rock} = 0.2\ \mu A/m^2$. The plasma vortex is formed at early time and plasma bubble at later time. (b) Contour plots of ΔTEC during formation of plasma vortex. (c) Contour plots of TEC during formation of plasma bubble.

Lithosphere-Magnetosphere: a possible coupling mechanism

Van Allen Belts

VLF waves interact with Van Allen belts particle, change pitch angle and lower mirror points

VLF waves propagation into the ionosphere

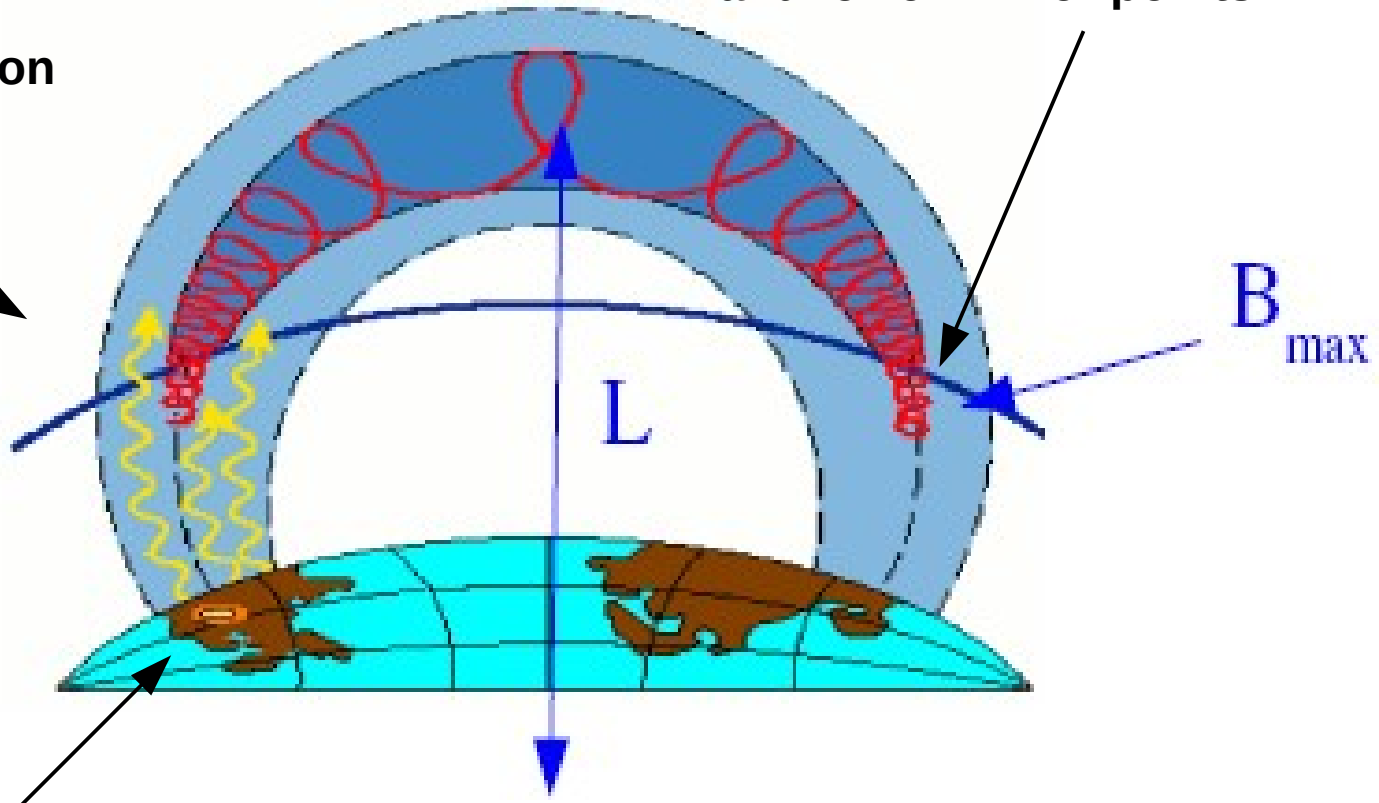

Earthquake preparation area

The particle perturbation propagates: latitude bouncing longitude drifts

Lithosphere-Magnetosphere: a possible coupling mechanism

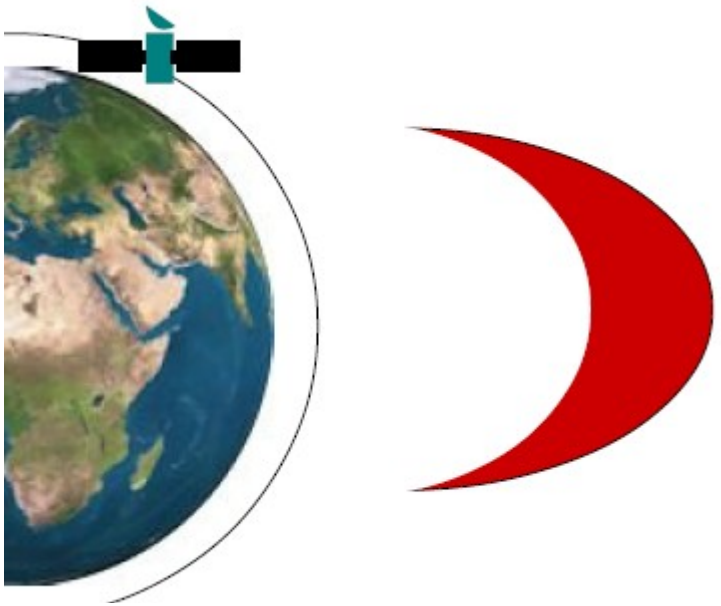

After the lowering of mirror points the perturbed belt can be detected by a satellite on a lower orbit as a sudden increase in the particle count rate

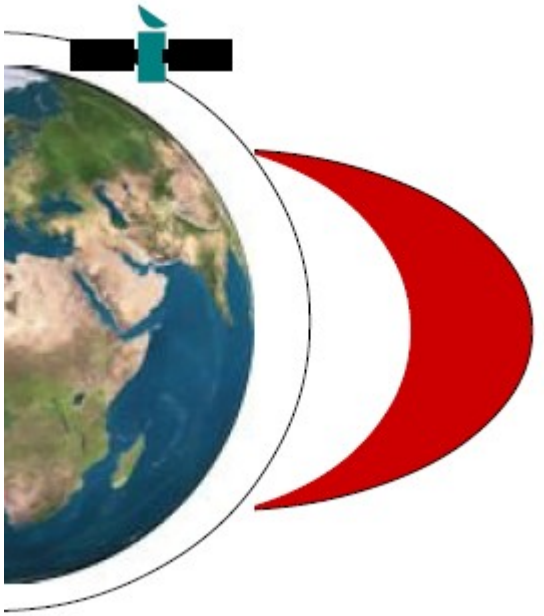

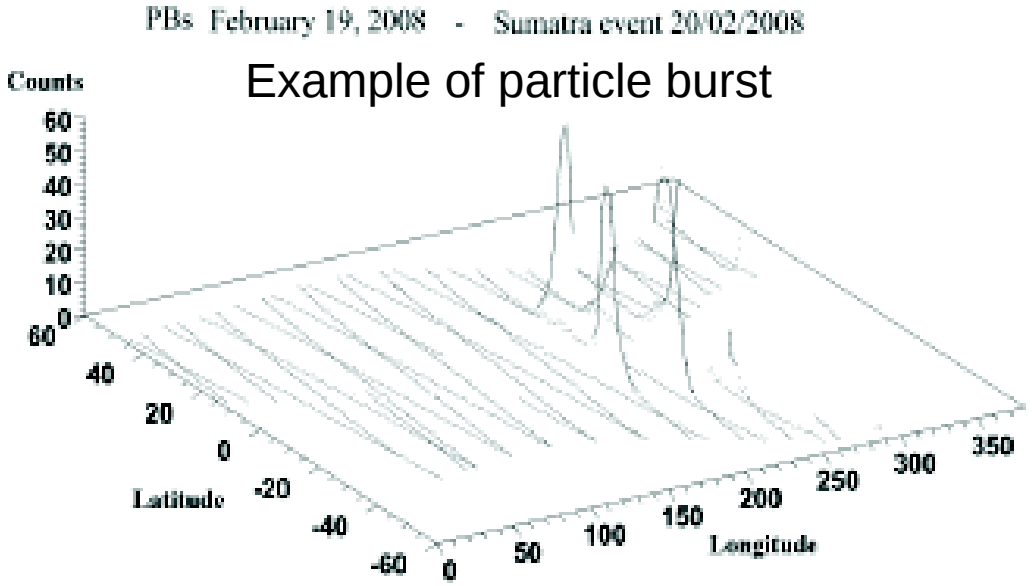

Example of particle burst

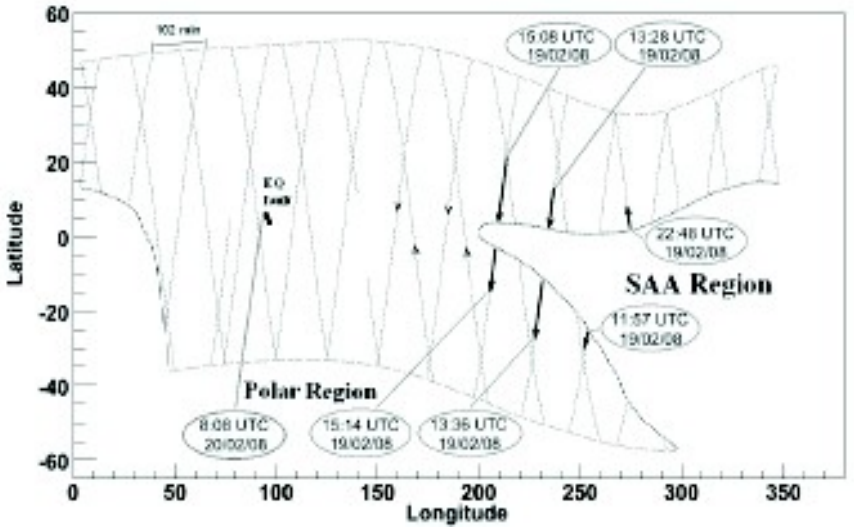

C. and Battiston R., 2008, NHESS 8, 1277

A test of the VLF-belts interaction

GEOPHYSICAL RESEARCH LETTERS, VOL. 35, L09101, doi:10.1029/2008GL033194, 2008

Radiation belt electron precipitation due to VLF transmitters: Satellite observations

J.-A. Sauvaud,[1] R. Maggiolo,[1] C. Jacquey,[1] M. Parrot,[2] J.-J. Berthelier,[3] R. J. Gamble,[4] and Craig J. Rodger[4]

- CNES-CNRS mission **DEMETER** (Detection of Electro-Magnetic Emissions Transmitted from Earthquake Regions) June 2004-Dec 2010,
- Combined wave and particle observations from the DEMETER satellite
- ICE: electric field ULF-VLF measurements
- IDP: electron flux 60-600keV
- Injection of e.m. waves with the NWC ground-based transmitter
- Found enhancements in the 100–600 keV drift-loss cone electron fluxes directly linked to NWC operation and ionospheric absorption.

A test...

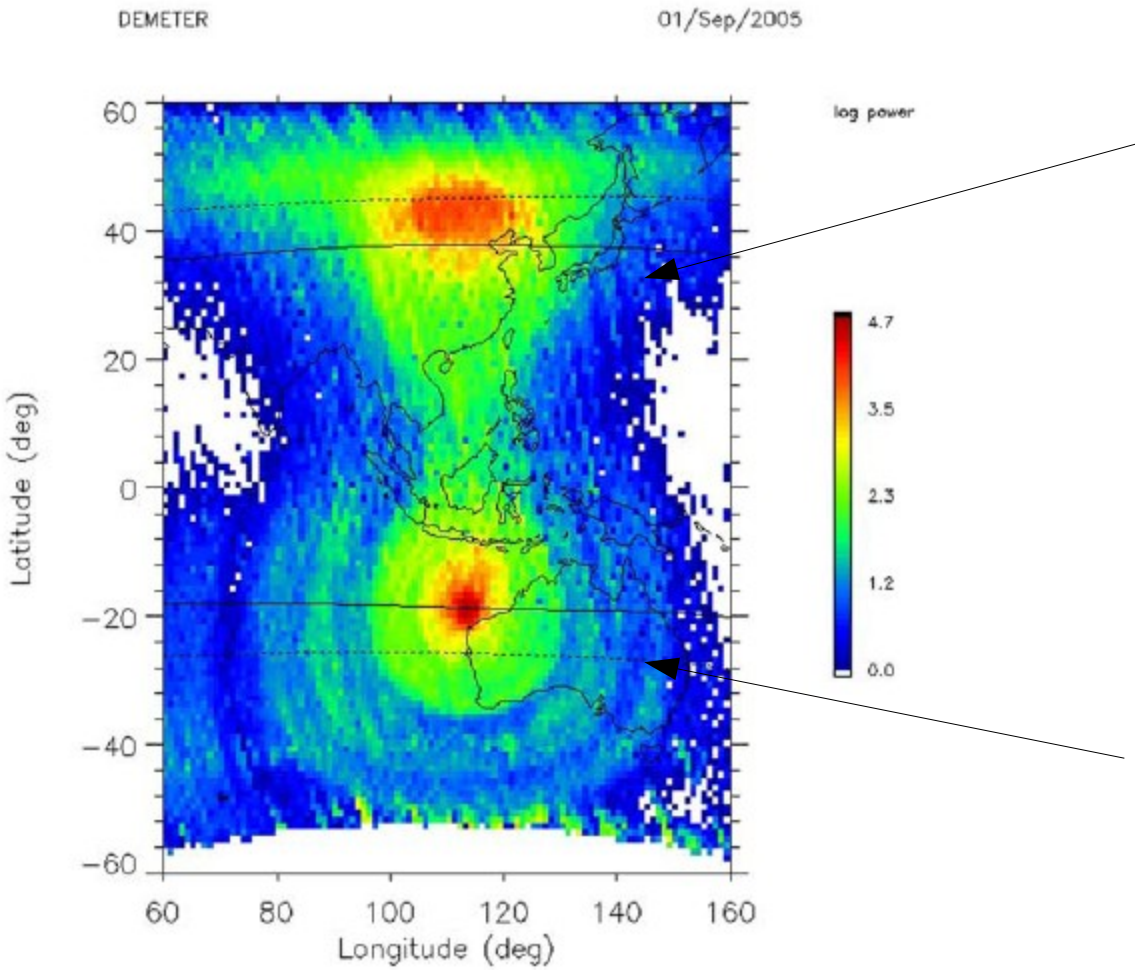

Japan

Australia

Figure 1. Geographic display of the average power received by the ICE instrument on DEMETER from the NWC transmitter at 19.8 kHz. L-shell contours computed at the satellite altitude (700 km) are also shown (L = 1.4 and L = 1.7). In a large region around the transmitter, there are interferences of the VLF modes. The wave power is given in $\mu V^2/(m^2.Hz)$.

A test of ....

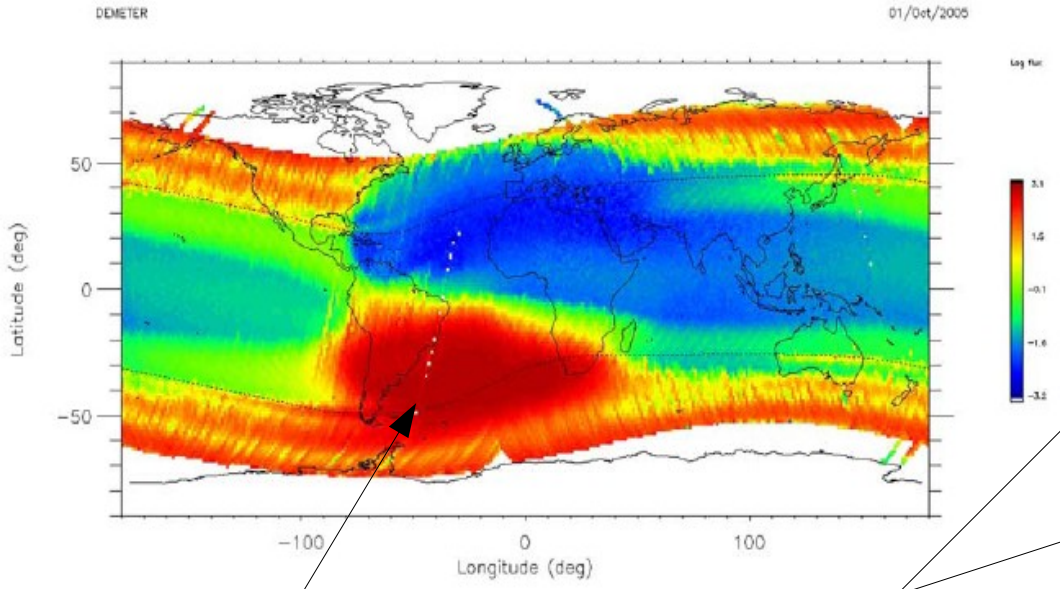

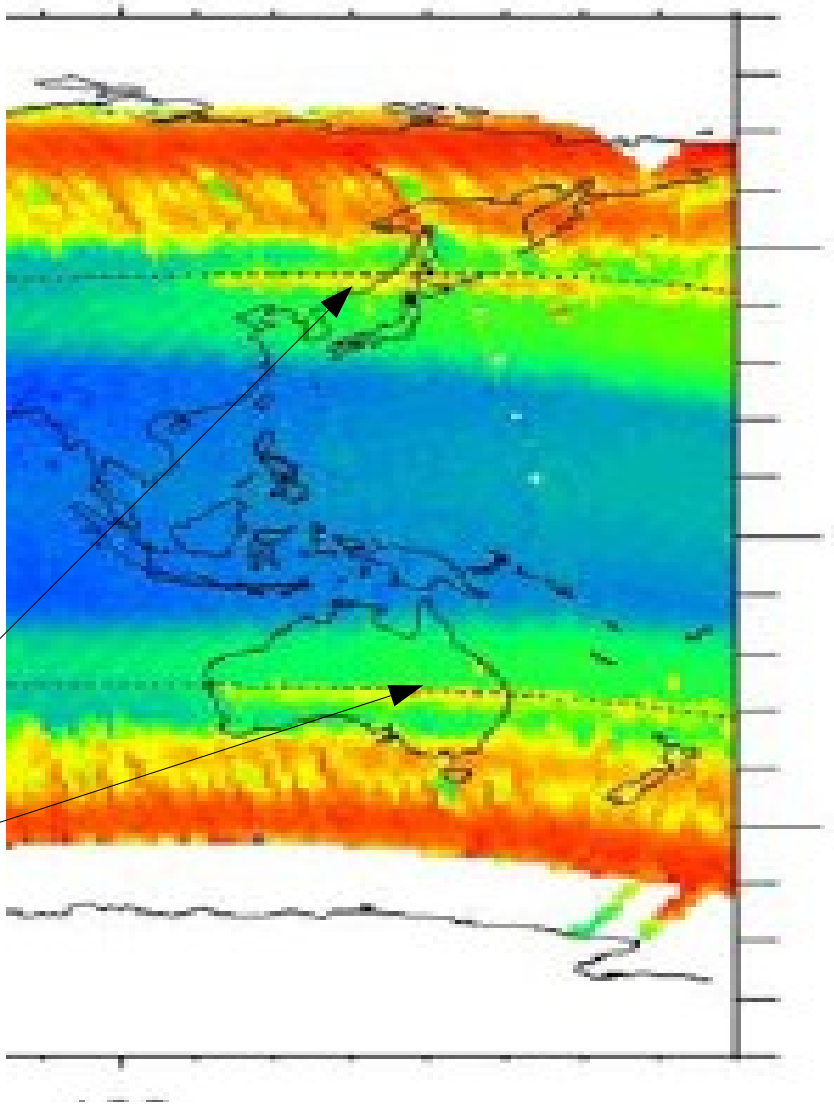

SAA

Induced precipitation

Figure 2. Geographical distribution of quasi trapped electron fluxes at an energy of 200 keV. The L = 1.7 contours, computed at 700 km altitude, are also shown. Note the large flux enhancement inside the South Atlantic Anomaly and its counterpart with weak fluxes in the Northern Hemisphere. At the highest magnetic latitude ($\sim\pm65^\circ$), the satellite encounters the auroral zones. The outer radiation belt is detected at all longitudes, at latitudes ranging from -45° (-180° longitude) to -60° (-90° longitude). On the contrary, the electron structure associated with NWC is only detected from the west coast of Australia eastwards and follows the L (= 1.7) contours as expected from the electron drift motion. Fluxes are given in $e^-/(cm^2.ster.keV)$.

Early measurements of MeV electrons

Annales Geophysicae (2003) 21: 597–602 © European Geosciences Union 2003

High-energy charged particle bursts in the near-Earth space as earthquake precursors

S. Yu. Aleksandrin[1], A. M. Galper[1], L. A. Grishantzeva[1], S. V. Koldashov[1], L. V. Maslennikov[1], A.M. Murashov[1], P. Picozza[2], V. Sgrigna[3], and S. A. Voronov[1]

- 1980s-90s missions for trapped particle studies
- **MARIA-MARIA2** (SALYUT 7) electrons 20-200MeV
- **ELECTRON** (METEOR 3) electrons >30MeV
- **GAMMA**, electrons >50MeV
- **SAMPEX**/PET electrons 4-15 MeV
- They found electron bursts, and search for time correlation with powerful Eqs
- In the time-difference distribution an excess is found at 4.0hours

Early measurements of MeV electrons

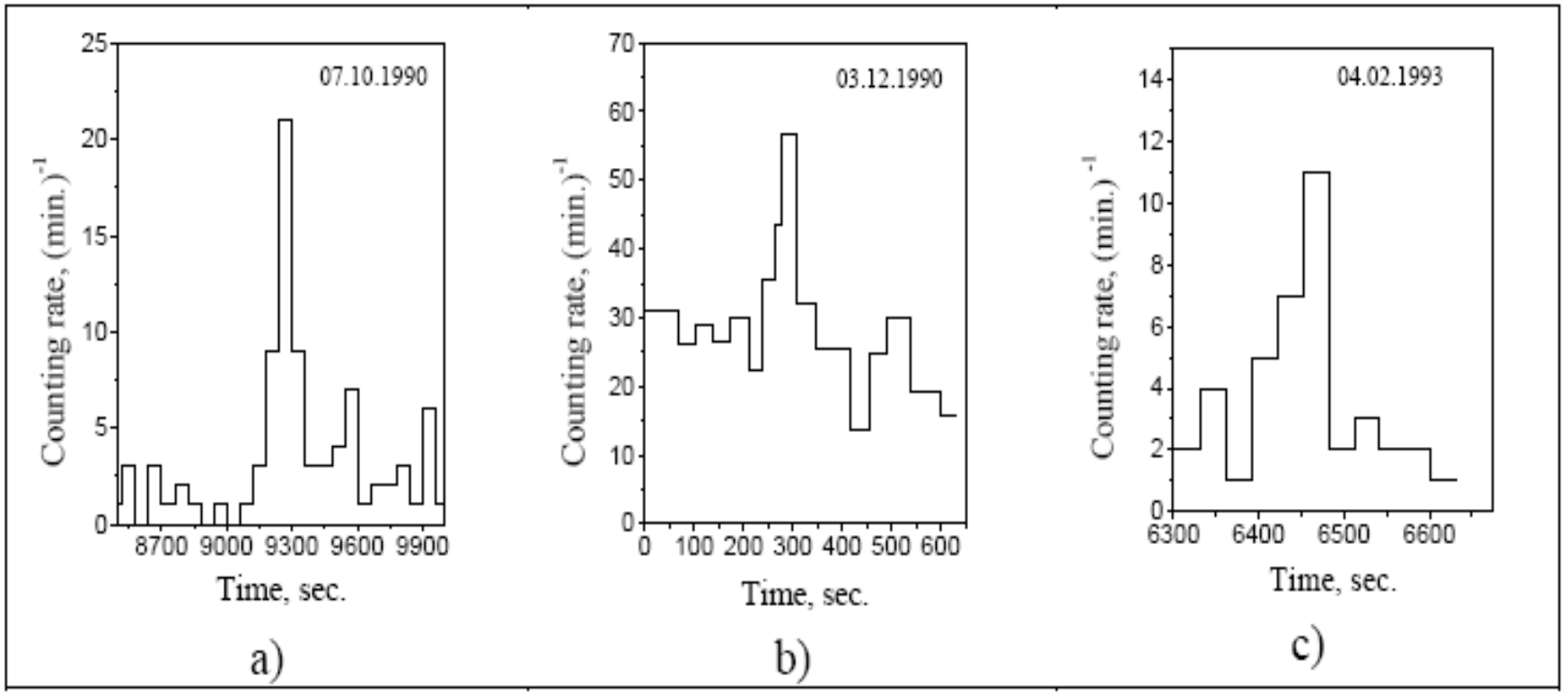

Fig. 1. Examples of electron counting rates along the orbit recorded in MARIA-2 **(a)**, GAMMA-1 **(b)** and SAMPEX/PET **(c)** experiments during observation of the particle bursts.

Typical MeV electron burst

Early measurements of MeV electrons

Main parameters for event selection

Eq Magnitude

$$\Delta L = L_{EQ} - L_{PB}$$

Note: one has to associate a L shell to the Earthquake
L_{EQ} = L coordinate at a given **COUPLING HEIGH** above the epicenter

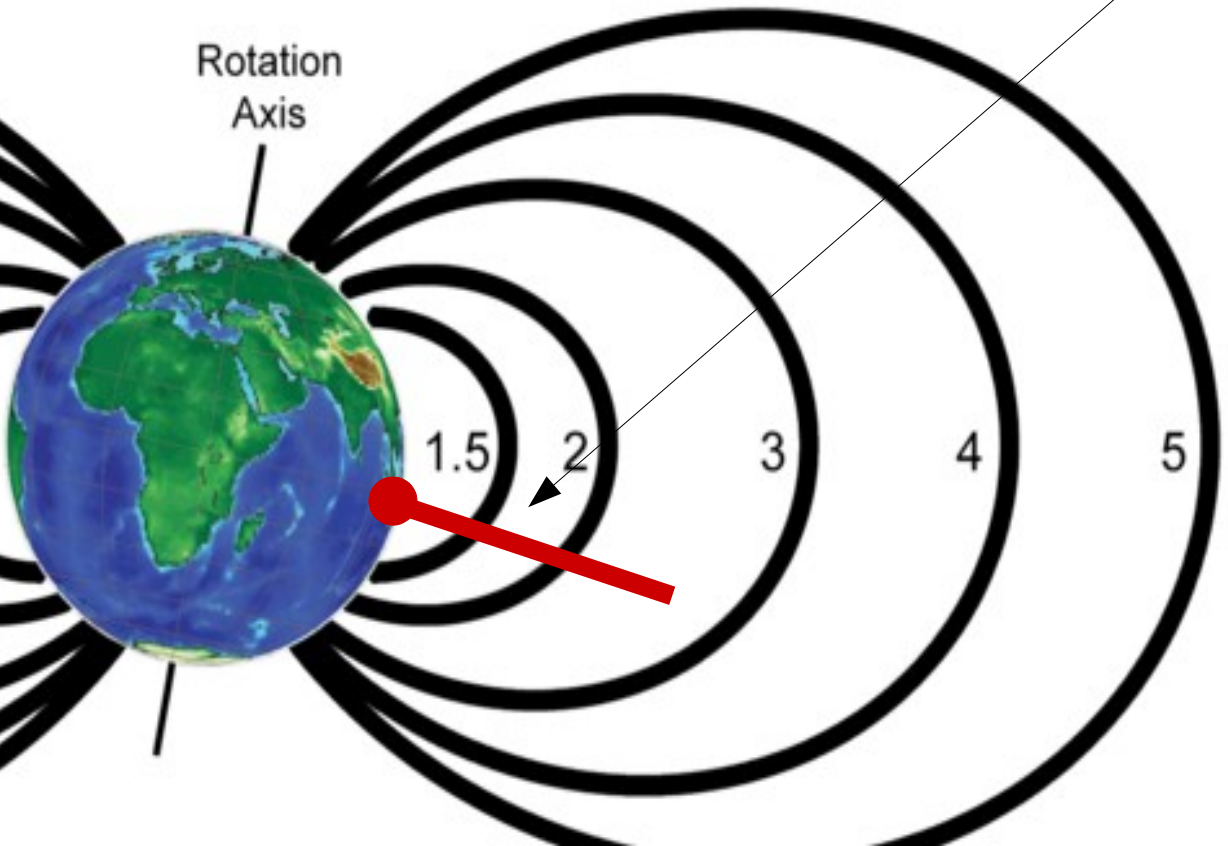

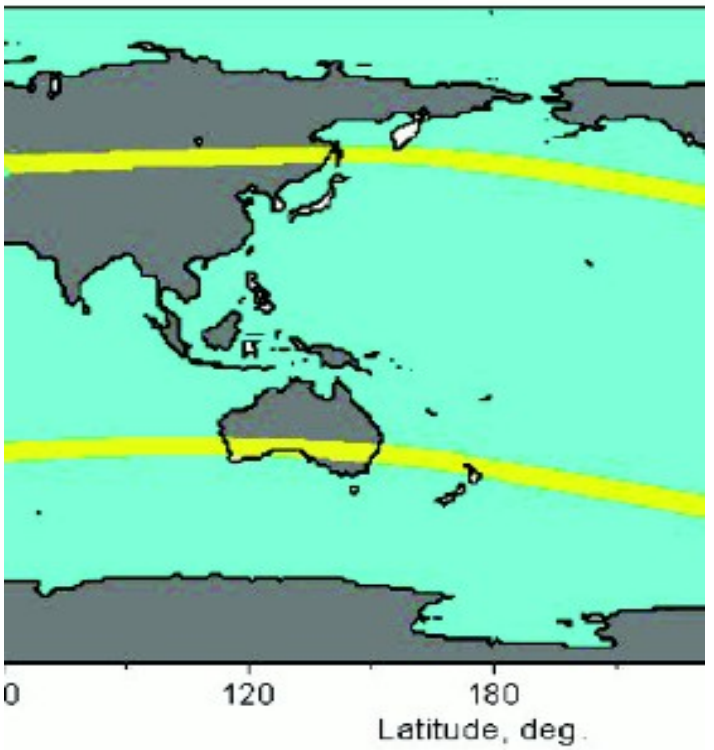

Early measurements of MeV electrons

Time correlation: the time difference between the considered electron bursts and Eqs

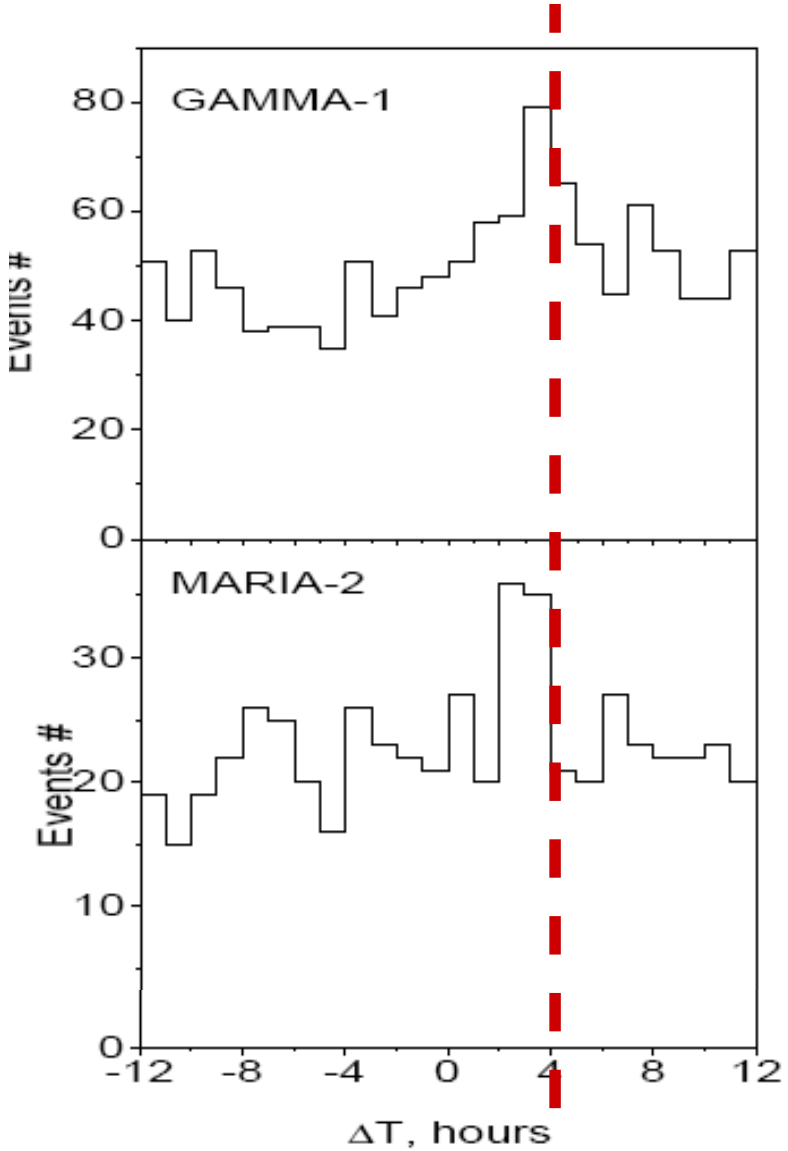

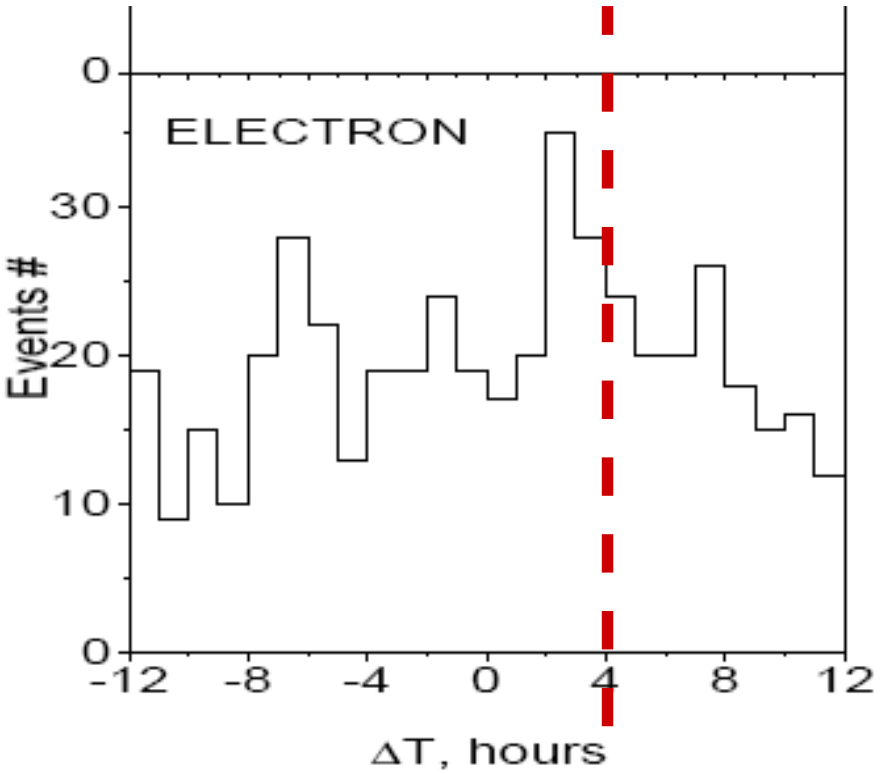

Fig. 2. ΔT distribution histograms for particle bursts and earthquakes obtained in GAMMA-1, MARIA-2, PET and ELECTRON experiments ($M > 4$, $|\Delta L| < 0.1$).

Early measurements of MeV electrons

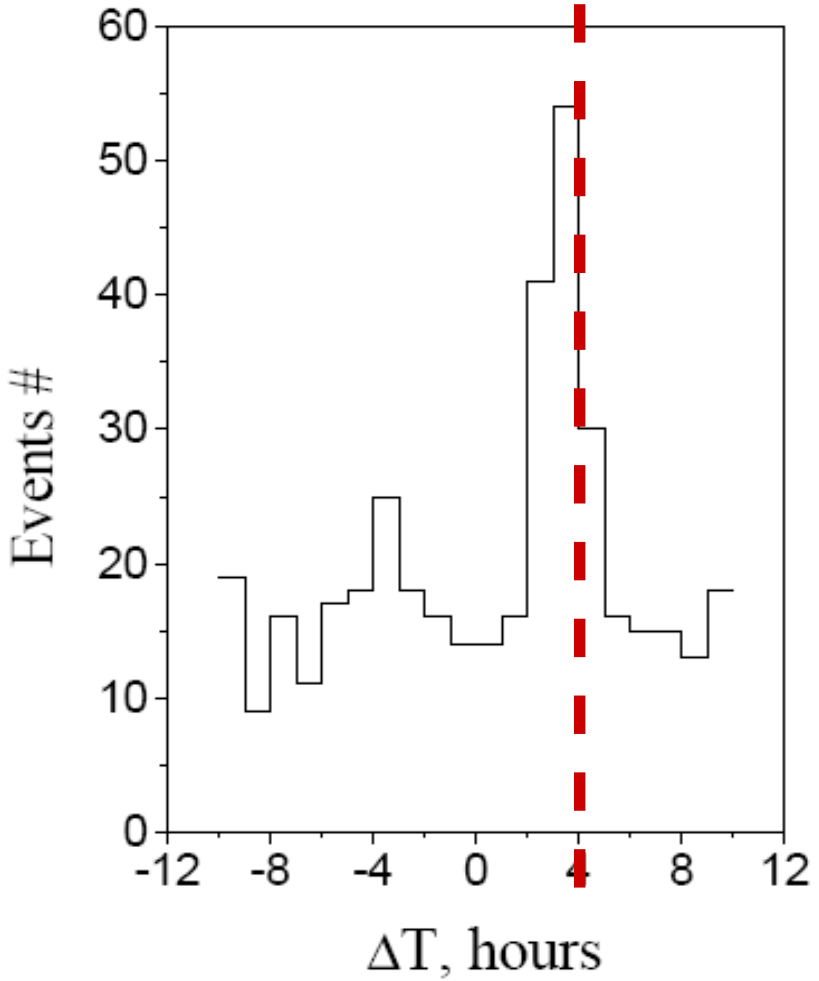

Fig. 3. ΔT distribution histogram for particle bursts and earthquakes (SAMPEX/PET, $M > 5, |\Delta L| < 0.07$).

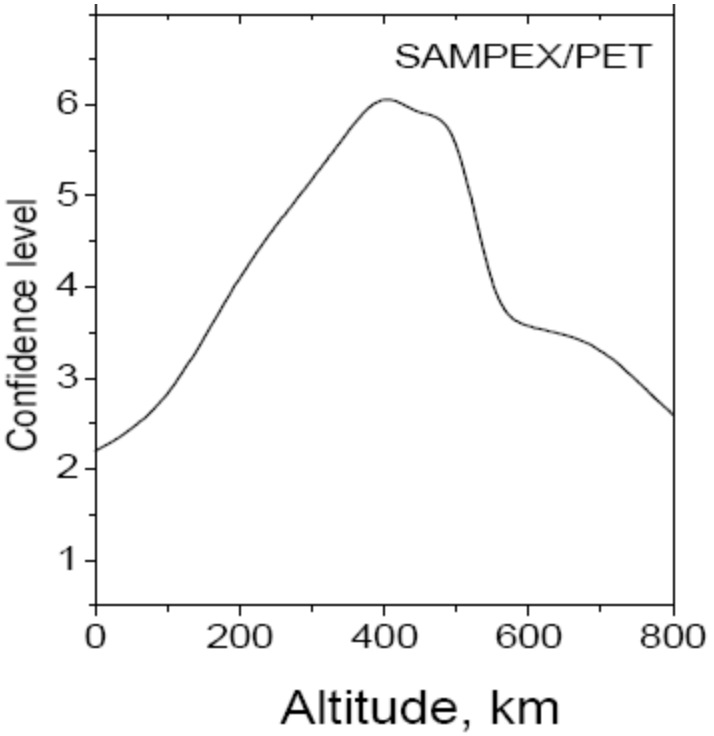

Fig. 5. Confidence level (in number of standard deviations) of the peak in the ΔT distribution histograms vs. assumed value for the altitude of EME capture in a geomagnetic field tube (MARIA-2, GAMMA-1 and SAMPEX/PET).

They optimized the results for the Coupling height

New SAMPEX data analysis

Journal of Atmospheric and Solar-Terrestrial Physics 67 (2005) 1448–1462

Correlations between earthquakes and anomalous particle bursts from SAMPEX/PET satellite observations

V. Sgrigna[a], L. Carota[b], L. Conti[a,*], M. Corsi[a], A.M. Galper[c], S.V. Koldashov[c], A.M. Murashov[c], P. Picozza[d], R. Scrimaglio[b], L. Stagni[e]

- New analysis of the SAMPEX/PET data
- They found difference related to the operational mode of the instruments (ORR,MOR,RPM modes)
- They found correlation between EQ and electron busts in the energy range 4-15MeV, at 4.0hours

New SAMPEX data analysis (II)

Table 2
PET channel Level-2 data available for the study

Particles	Energy (MeV)	Geometric factor (cm^2 sr)	Channel
Protons	28–60	1.5	PHI
Protons	19–28	1.65	PLE
Electrons	2–6	1.65	ELO
Electrons	4–15	1.5	EHI
Electrons	4–30	—	EWG
Protons	>60	0.4	RNG
Electrons	>15		
Protons	>85	0.25	PEN
Electrons	>30		

Table 1
Main characteristics of the SAMPEX/PET mission

Orbit altitude	520–670 km
Orbit inclination	82°
PET Pointing modes	ORR, MORR, 1 RPM (see text)
Time interval under study	from July 1992 to December 1999

The used data, approx 1 year

New SAMPEX data analysis

CRs = particle flux measurements integrated over 30 s

CR daily background matrix $\{L,\alpha_{PET}\}$:

$1.0 \leqslant L_{PB} \leqslant 1.8$ (L-step = 0.1)

$0^\circ \leqslant \alpha_{PET} \leqslant 180^\circ$ (α_{PET} – step = 15°)

Poissonian cut: $p < 0.01$

No measurements in the SAA region

$A_p < 20$

SID = 0

Burst Search in Cells

Spurious Background filtering

L_{eme}: supposed VLF waves-particle coupling height

EQ–PB correlation

$H_{MIRR} \approx 400-900$ km

$|H_{MIRR} - H_{SAMPEX}| > 30$ km

$\Delta L = L_{EME} - L_{PB} < 0.1$

$\Delta T_{MAX} = (T_{EQ} - T_{PB})_{MAX} = \pm 3$ days

New SAMPEX data analysis

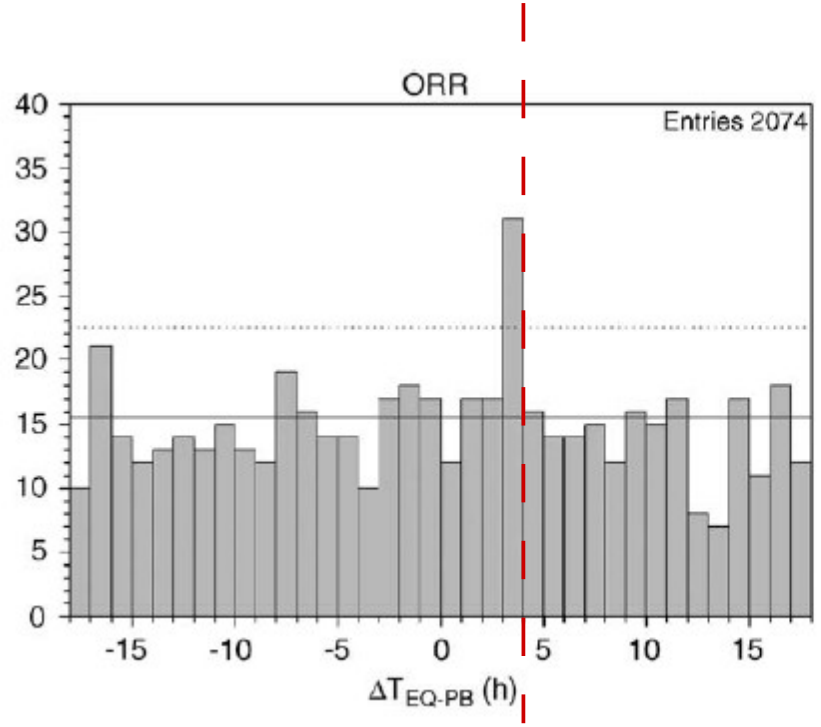

Fig. 4. Histogram of the $\Delta T_{\text{EQ-PB}}$ temporal correlations between PBEHI and EQs for the ORR PET-pointing mode. Only during this pointing period, a significant peak is evident at $\Delta T = 4$ h, demonstrating that only in this case PBs statistically precede EQs, thus indicating a preseismic character. A time window of 18 h has been used only for graphical representation. The horizontal solid and dotted lines indicate the mean amplitude of each distribution and the mean + 2 standard deviation units, respectively.

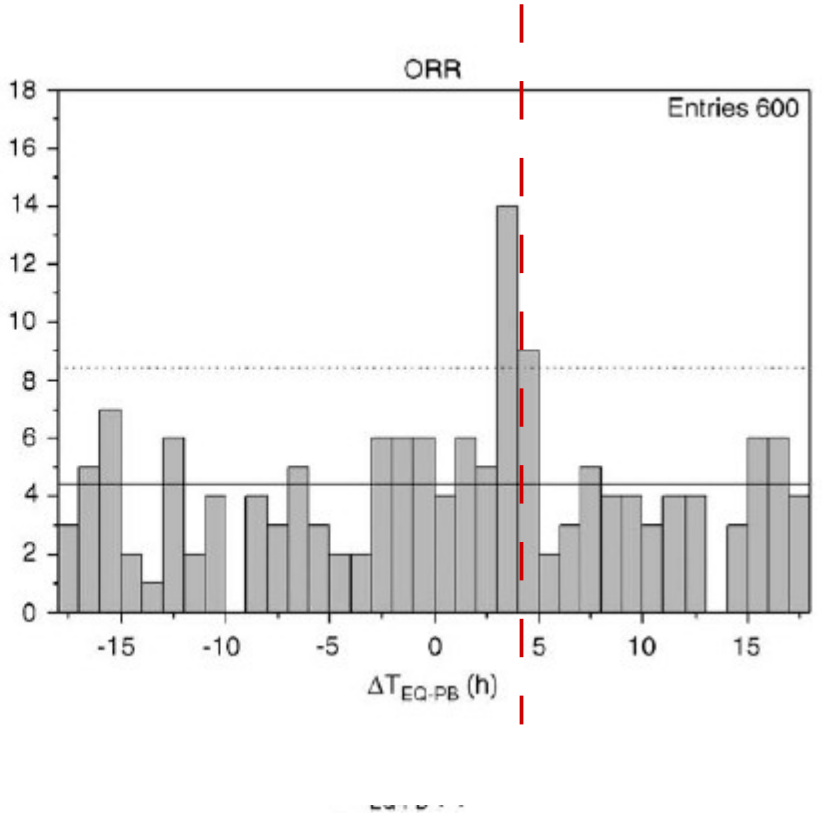

Fig. 5. Histogram of the $\Delta T_{\text{EQ-PB}}$ temporal correlation between EQs and PBEHI data (detected at $\alpha_{\text{PET}} < 70°$ and $\alpha_{\text{PET}} > 110°$) for the ORR PET-pointing period. As in Fig. 4, also in this case, but with a better signal-to-noise ratio, a peak is evident at $\Delta T = 4-5$ h only with data collected during the ORR-pointing mode, indicating that PBs statistically precede EQs, i.e., PBs exhibit a preseismic character. The horizontal solid and dotted lines indicate the mean amplitude of each distribution and the mean + 2 standard deviation units, respectively.

ARINA

A.M. Galper, Erice, Italy, 23 October 2012

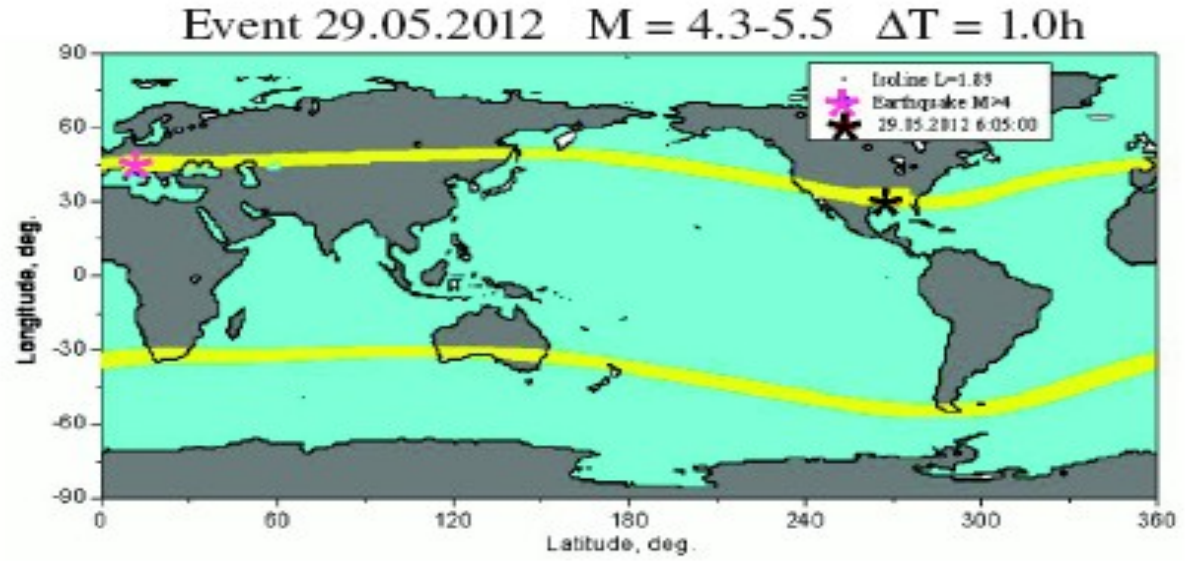

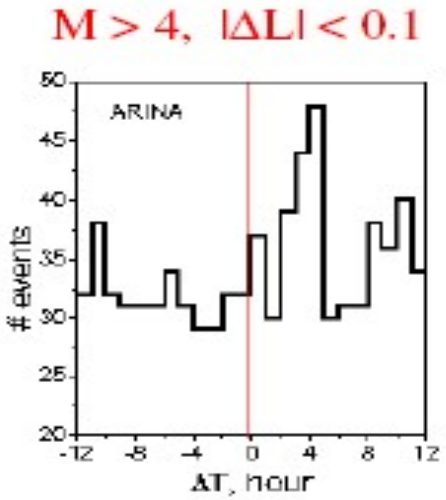

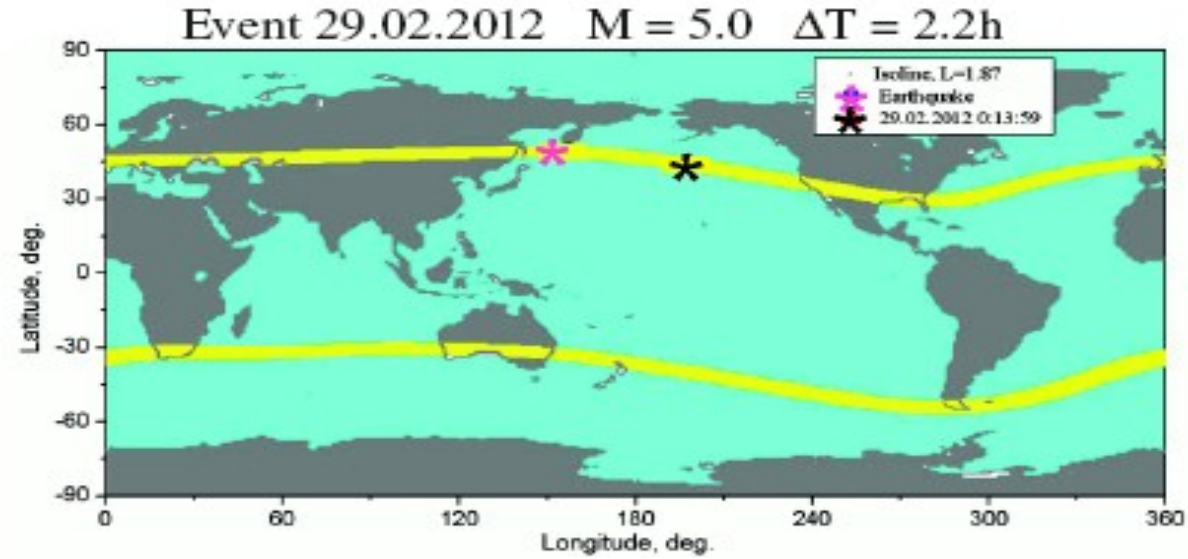

The ARINA spectrometer measures proton and lepton (electron and positron, without charge separation) fluxes in energy ranges 4-30 MeV for leptons and 30-100 MeV for protons.

Current Studies: POES Satellites

- We searched for correlations between low energy electrons (E > 0.3 MeV) precipitation and earthquakes with magnitude above 5 Richter scale
- NOAA Polar Orbit Environment Satellites 15-16-17-18(-19)
- We used a large data sample:
  the electron data of POES 15,16,17 and 18 satellites collected during 13 years
  18 thousands M>5 earthquakes in the NEIC catalog of the U.S. Geological Survey
- Relatively low energy electrons
- Very good time and space coverage

.

Current Studies: POES

- Medium Energy Proton and Electron Detector (MEPED) on board of POES satellites
- 8 solid-state detectors for protons and electrons in an energy range from 30 keV to few hundreds MeV.
- Electrons detectors: 700 μm thick silicon devices:
  25mm2 sensitive area;
  ±30deg opening angle collimator;
  0.1 cm2sr geometric acceptance;

detectors channels	energy range keV	contaminants
e1	30-2500	210-2700keV protons
e2	100-2500	280-2700keV protons
e3	300-2500	440-2700keV protons
p1	30-80	
p2	80-240	
p3	240-800	
p4	800-2500	
p5	2500-6900	
p6	>6900	>700keV electrons
$p6_{omni}$	>16000	>800keV electrons
$p7_{omni}$	>36000	

Table 2. MEPED Telescopes Parameters.Electron detectors have energy channels identifier starting with *e*, protons detectors with *p*. In the second columns is shown the channel energy range while in the third the known contaminants. Data are taken from [25] and [27].

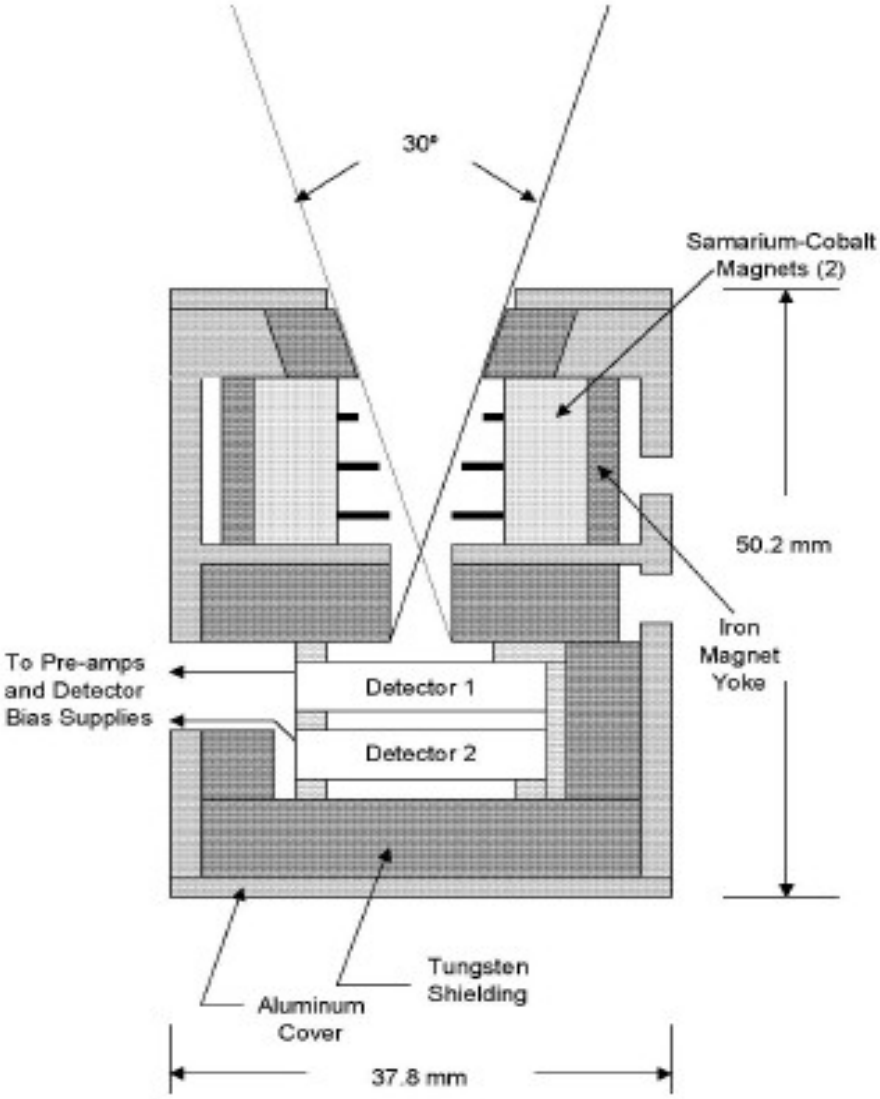

POES data analysis

- First analysis step: search for Particle Burst
- Search for Particle Burst in three-dim (time-L-pitch)
- For each cell the Particle Burst (PB) defined as electrons counting rate having a probability <1% to be a background fluctuation
- SAA excluded with a condition on magnetic field
- All the geomagnetic field related quantities calculated with IGRF as a function of the time

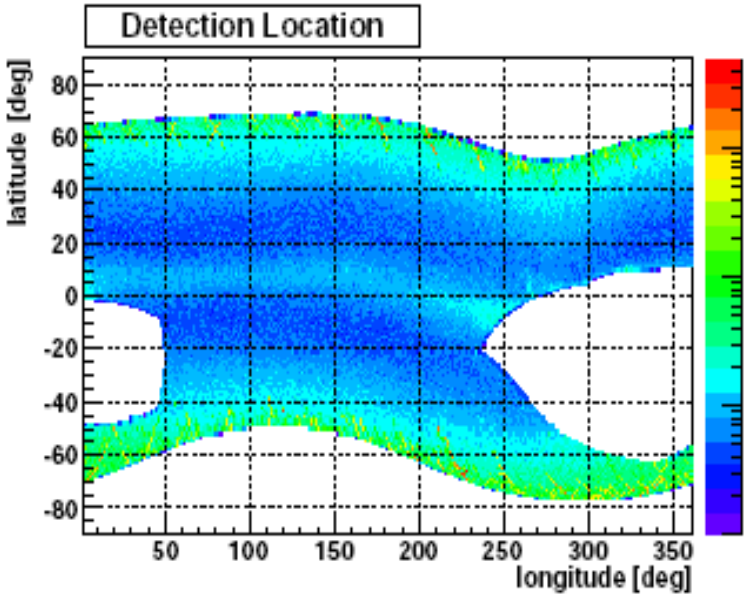

Fig. 2. Detection Locations. Here are reported the geographic locations at which the rates measurements in Figs 1 and 2 were performed. It is visible the rejection of the South Atlantic Anomaly region.

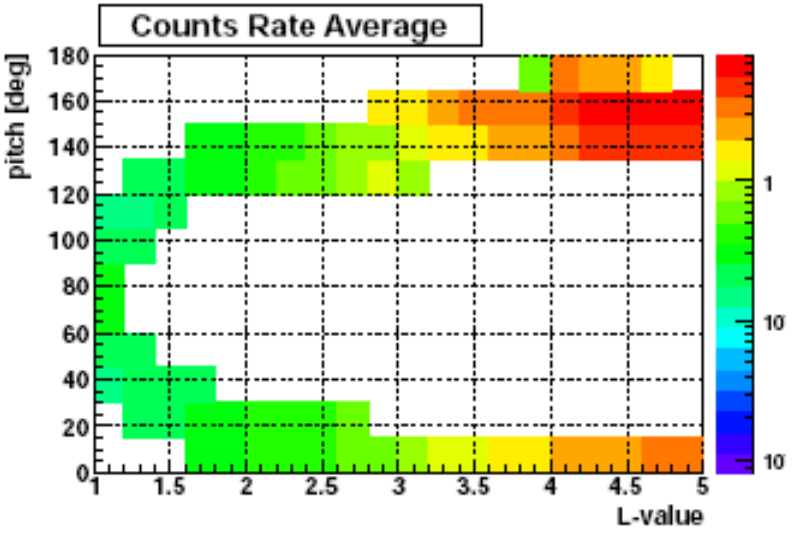

Fig. 1. L parameter-pitch angle Phase Space. Here in colour code the average count rates (particle s^{-1}) for each of the used L parameter-pitch angle cells are reported. The integration time is of one year instead of 1 day, as used in for the analysis,in order to illustrate the phase space.

POES data analysis

- Second step: search for Composite Bursts(CB):
  Single Particle Burst very close in time are grouped
- Event selection:
  (I) each CB should have a conjoint in the opposite hemisphere
  (II) Delta L (Mc Laughlin) between Earthquake and CB should be < 0.1
  (III)Spurious Events filtering (Ap and SID)
- Then Time Correlation distribution

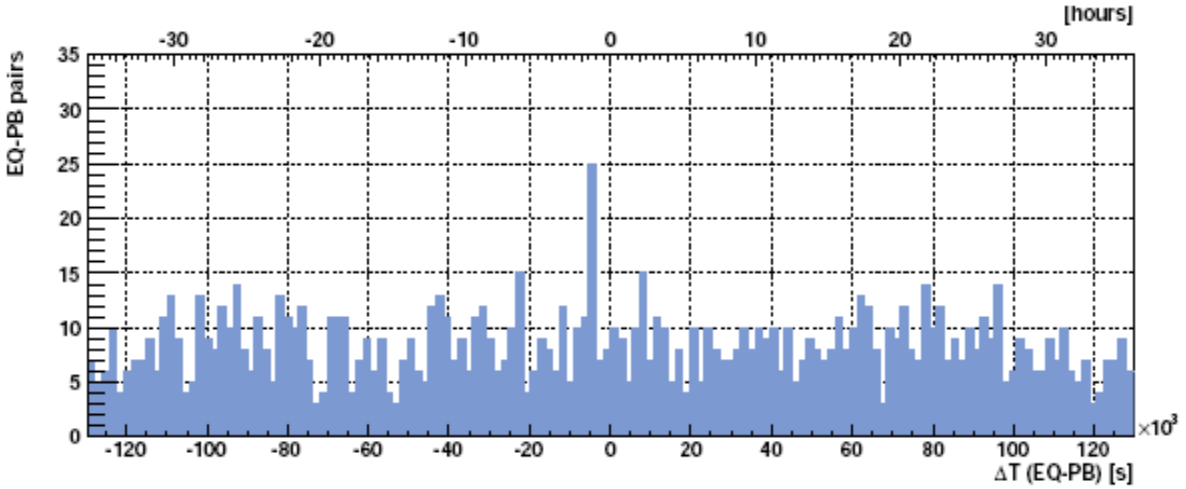

Fig. 3. The Time Difference Distribution. Here the time delays between the seismic events and the selected particle bursts are ploted. EQ-PB pairs are taken within a time window of ±1.5 days. This distribution is uniform within the statistical errors but with an excess at -1.25±0.25 hours. On the inset a zoom of the Time Difference Distribution between 0.5 and 2 hours is reported.

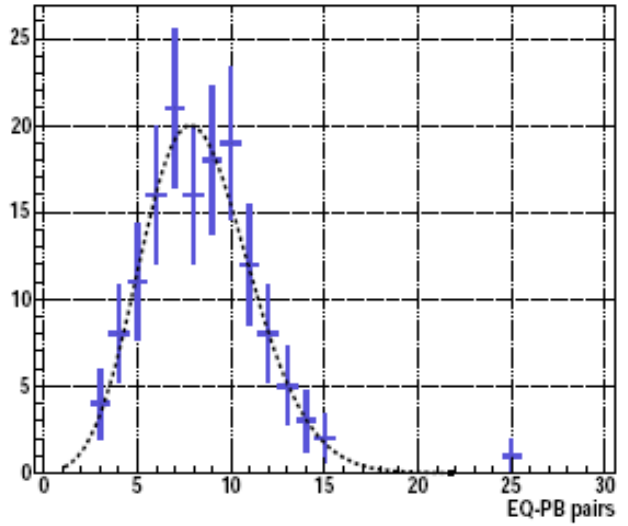

Fig. 4. The EQ-PB Pairs Distribution. Here the number of EQ-PB pairs in each time bin in Fig 3 are plotted. The number of pairs distribute in agreement with a Poisson distribution, with a mean value μ = 8.33±0.27. The excess counts value is at 25. This value deviates 5.7 standard deviation ($\sqrt{\mu}$=2.886) from the distribution mean and has a probability of $1.2*10^{-6}$ to be part of the main distribution.

POES data analysis

Satellite	C	μ	$(C-\mu)/\sqrt{\mu}$
15	7	3.25±0.19	2.08
16	7	2.00±0.16	3.53
17	7	2.21±0.13	3.23
18	4	0.98±0.12	3.05

Table 5. Contributions of each satellite to the excess. The columns correspond to the satellite identification, to the number of counts in the -1.25 hours bin (C),the mean value of in the Δt distribution (μ) and the significance of the counts in the -1.25 hours bin $(C-\mu)/\sqrt{\mu}$

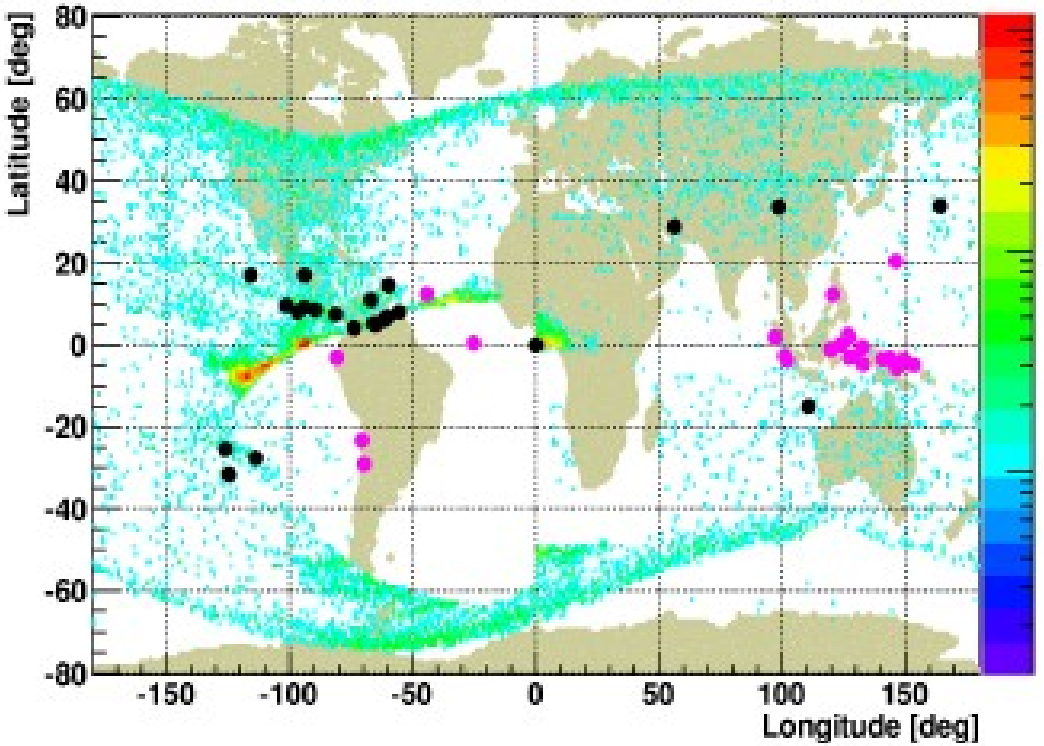

Fig. 5. The Geographic Distribution of Correlating Seismic Events and Electron Bursts. Here are shown as color code the distribution of all CBs and the CBs (as black dots) and the earthquakes (as purple dots) with time delay in the range of -1.25±0.25 hours.

POES data analysis

- Evidence for a correlations between earthquakes and particle bursts has been found
- only using the highest energy bin (E>300 keV) of the zenith pointing (0deg) MEPED electron telescope (no lower energy, no protons)
- The relatively low energy of the electrons and small geometric factor of the detector might explain the small efficiency of the search
- **NOTE**: In the case of 300keV electrons with L parameter of 1.3, the drift velocity is in the order of 2.7 km/s, namely their total drift period around the earth takes four hours. It follows that the observed correlation can be interpreted differently if, before being detected by the satellite, the particle burst would travel less or more than one orbit. In the first case the correlation is observed following the earthquake, while in the second case the perturbation event would anticipate the earthquake by about three hours
- A detailed **simulation of the Earth magnetic** field and particle **back-tracing** is needed.

Current Studies: SEPS

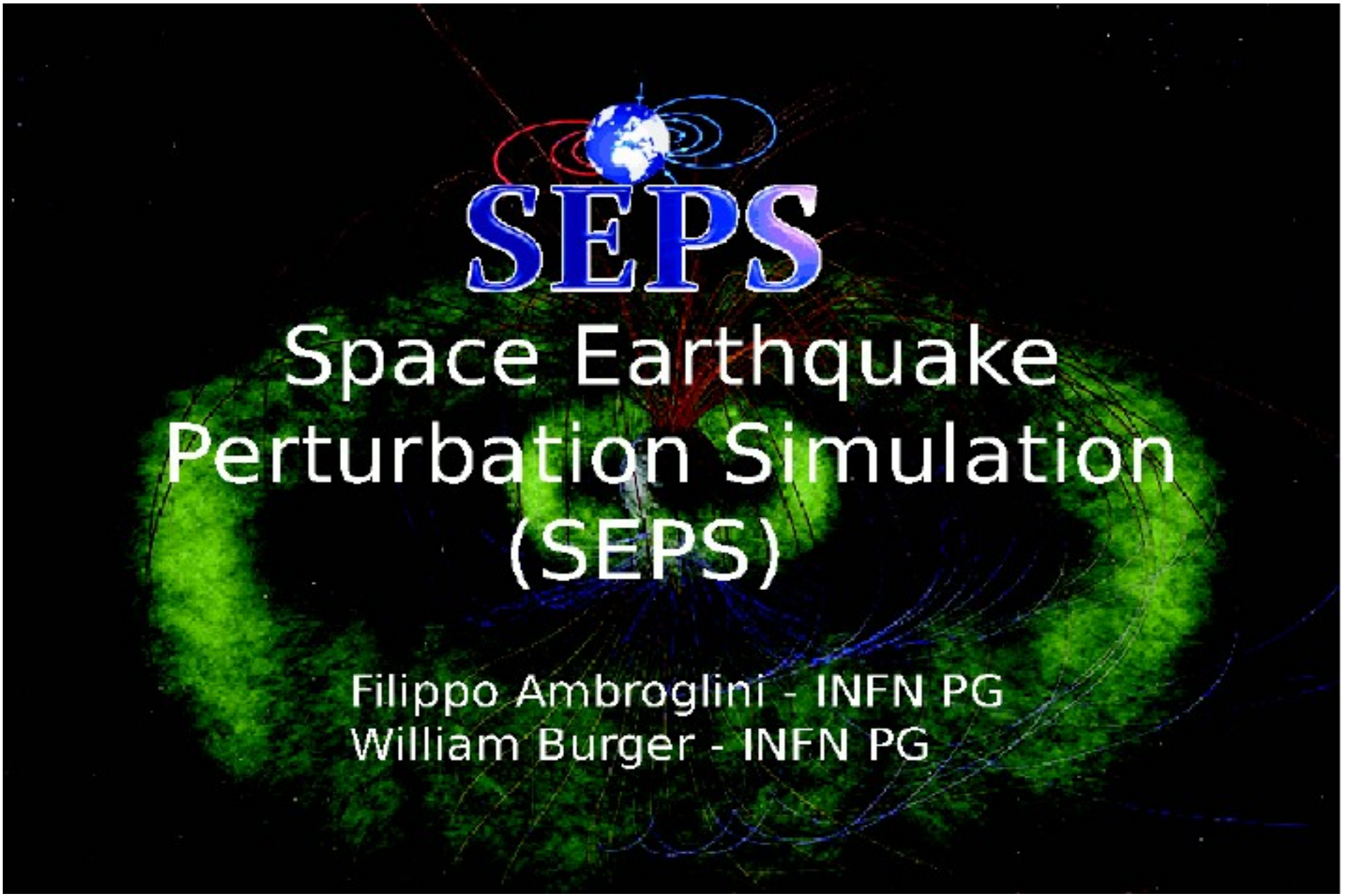

SEPS

A simulation code based on Geant4 and the PLANETOCOSMICS application that allow to simulate the interaction of the EM perturbation with the particle entrapped in the magnetosphere on a track by track basis.

IGRF model is used for the Earth's internal field. The external field may be added by choosing among the available Tsyganenko models.

The NRLMSISE00 model is used for the Earth's atmosphere.

AE8 (MIN, MAX, MINESA) particle flux model is used to define the kinematics of the particles

SEPS Approaches

Two Approaches in the Simulaton

Start at the epicenter

- modelisation of the wave-particle interaction with the inner radiation belt particles
- study the optimal location of the satellite with respect to the epicenter location

Start at the observed site of the particle burst

- check the compatible of the observation with the site of the time-correlated earthquake (back trace)
- determine if the observed electrons occupy a stable drift shell (forward trace)

SEPS example

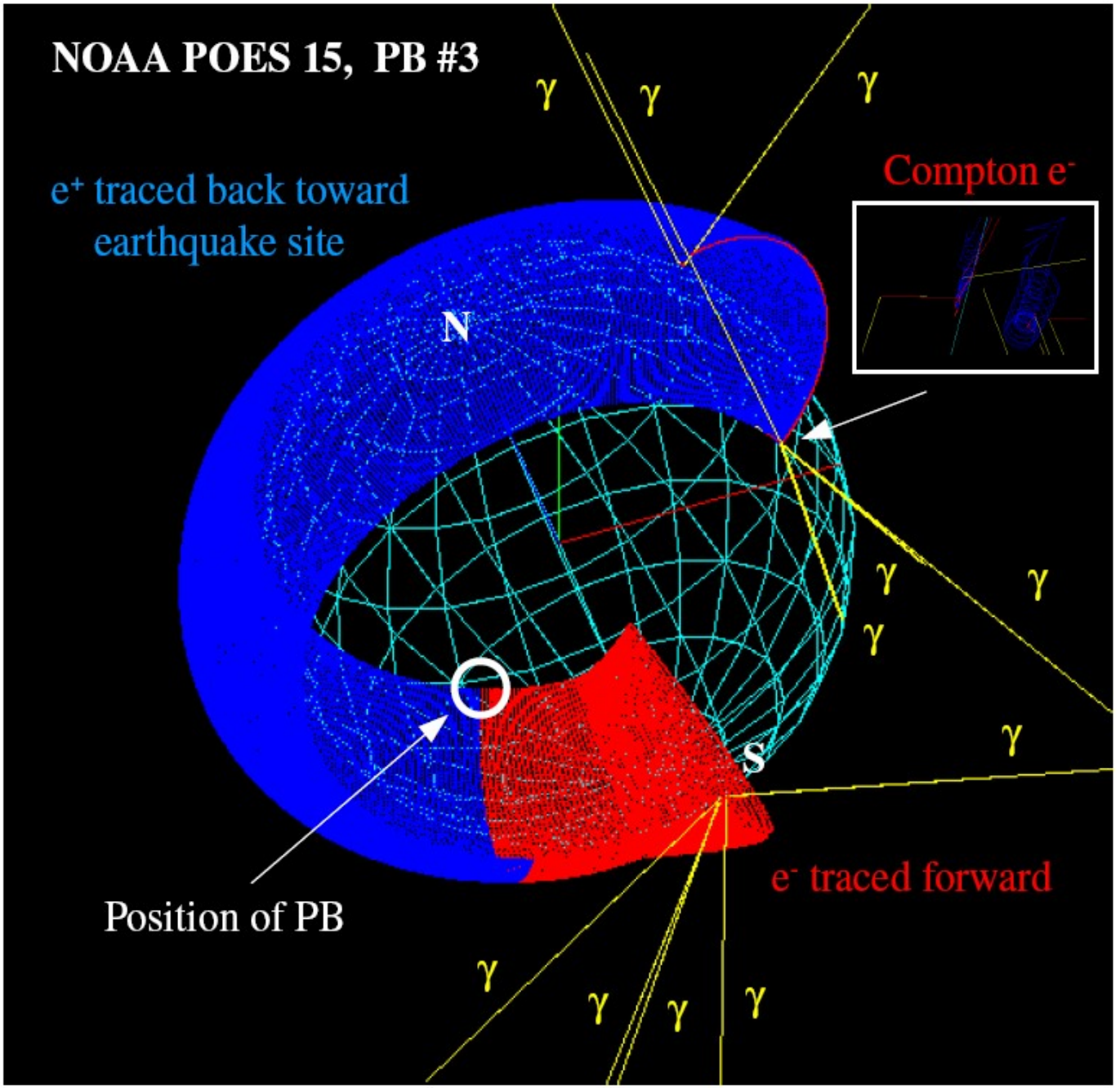

SEPS : results on POES data

- The event excess previously found has been analyzed with the back trace method.
- For each pair Earthquake-Particle Burst, it has been investigated the possibility to origin in the EQ location.
- The back trace inputs are:
  -Latitude, longitude and height of the satellite
  -FOV direction in respect of the local field line
- Among 25 events in the (delay plot) excess bin **16 can be originated from the correlated Eq location**.
- The left 8 pairs are compatible with the expected background
- The POES data analysis indicates the importance of the **local Pitch angle measurement**.

China Seismological Experiment Satellite (CSES)

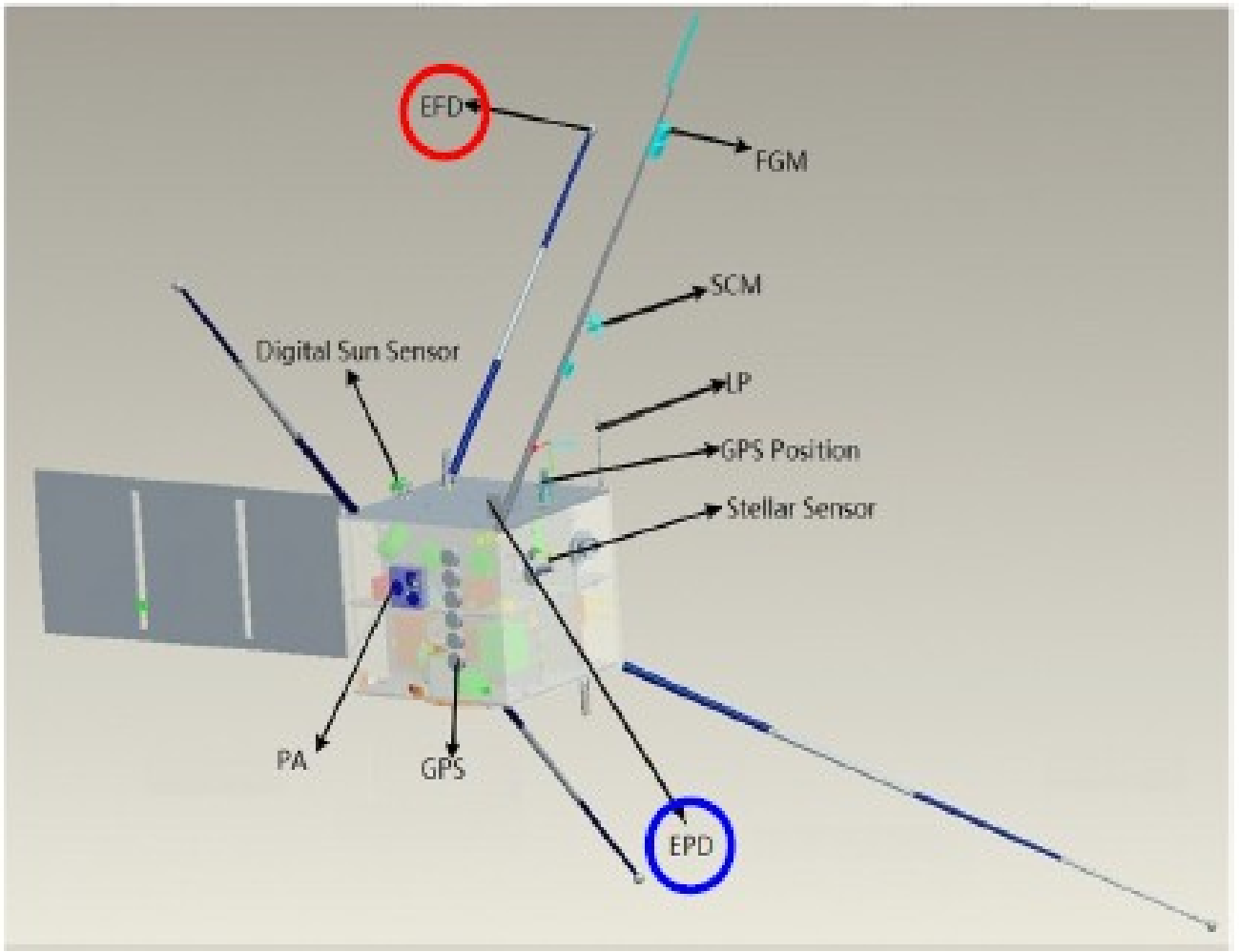

LEPD <0.110 MeV electrons (Institute of High Energy Phyiscs, CAS)
HEPD < 50 MeV el., < 500 MeV p (INFNBologna,INFNPerugia)
Electric Field Detector(INFNRoma,Tor Vergata, INFNRoma3, CISASPadova)

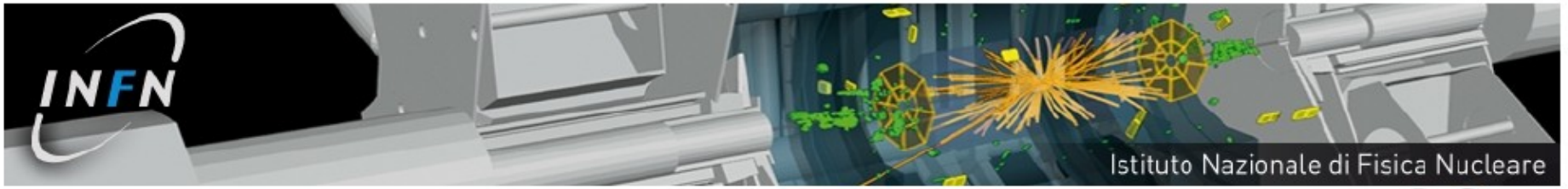

TERREMOTI, STRUMENTO INFN IN ORBITA

Pubblicato Mercoledì, 25 Settembre 2013 14:54

Uno strumento realizzato dall'INFN volerà con un satellite cinese per studiare le correlazioni tra alcuni fenomeni elettromagnetici e i terremoti. Un memorandum in questo senso è stato fimrato a Pechino dall'Agenzia Spaziale Italiana e dalla China National Space Administration: il protocollo d'intesa ha lo scopo di ospitare, per l'appunto, un payload italiano a bordo del satellite cinese CSES (China Seismo-Electromagnetic Satellite). Il principale obiettivo scientifico della missione è la ricerca su vari tipi di fenomeni di tipo elettromagnetico e la loro correlazione con fenomeni geofisici per contribuire al monitoraggio dei terremoti dallo spazio nel contesto delle Scienze della Terra. Diversi studi hanno evidenziato la possibile esistenza di correlazioni temporali tra emissioni elettromagnetiche legate all'attività sismica della Terra da una parte e il verificarsi di perturbazioni nel plasma iono-magnetosferico. L'Italia è sempre stata all'avanguardia in questo settore. Dal 2004 rapporti di regolare collaborazione tra i gruppi di ricerca Italiani dell'INFN guidati da Roberto Battiston presidente della commissione astroparticellare dell'INFN, e cinesi del CEA (China Earthquake Administration) hanno l'obiettivo di sviluppare la strumentazione di bordo del primo satellite cinese, chiamato CSES, dedicato allo studio dell'ambiente elettromagnetico attorno alla terra e dotato della strumentazione più avanzata esistente nel settore. L'Italia contribuirà al satellite CSES con uno strumento innovativo dedicato alla misura delle particelle energetiche che precipitano dalle fasce di Van Allen a seguito di disturbi elettromagnetici. Lo strumento Italiano sarà chiamato Limadou, in onore del famoso esploratore italiano Matteo Ricci e sarà realizzato dall'INFN nell'ambito di una collaborazione che vede coinvolti i centri INFN e le Università di Trento, Roma Tor Vergata, Perugia, Bologna e UniNettuno. La partecipazione dell'Italia al progetto CSES - ha dichiarato Roberto Battiston - prevede la realizzazione di un rivelatore di precisione per la misura degli elettroni che precipitano nell'atmosfera dalle fasce di Van Allen. In questo modo potremo sottoporre a verifica scientifica rigorosa i meccanismi che collegano il nostro pianeta e le sue dinamiche interne al plasma che circonda la terra, con l'obbiettivo di sviluppare nuove tecniche per il monitoraggio sismico dallo spazio".

Recent screenshot of INFN web-page with the news about the agreement between the Agenzia Spaziale Italiana and the China National Space Administration on CSES

CSES :The High Energy Particle Detector

PRIN05: Considerazioni per Il Rivelatore di Particella "L'Aiglon"

W.J. Burger, Perugia

Abstract

Electron and proton detection in the energy range from 1 MeV to 1 GeV has been studied with detector configurations based on momentum reconstruction and a total energy measurement. The expected angular resolution, which is provided by a tracking device common to the two types of detectors, is also reported. The acceptance is discussed in the context of a magnetic spectrometer.

The particle detector(s) determine the energy and direction (pitch angle) of the magnetically trapped electrons and protons encountered in the near-Earth orbit of the satellite. The energy resolutions obtained with momentum reconstruction and calorimetry have been evaluated with a Monte Carlo simulation. The detector configurations studied with Geant3 were: (1) a silicon tracker in a 1 kG field, (2) a silicon tracker (without magnetic field) and BaF_2 crystal calorimeter and (3) a scintillating-fiber tracker with the 1 kG field.

Currently also a version without magnet is under consideration

CSES:The High Energy Particle Detector

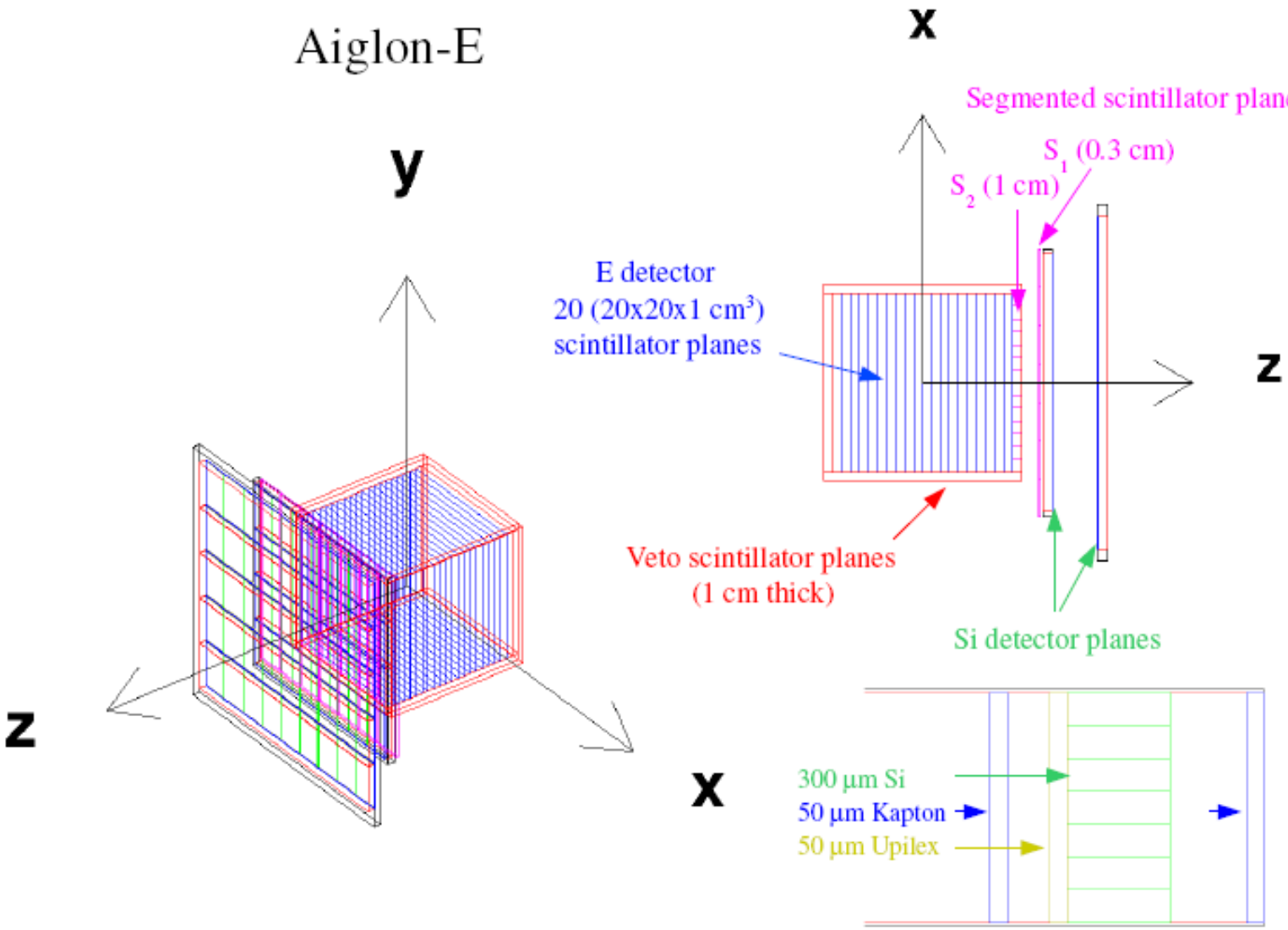

CSES:The High Energy Particle Detector

Angle Integrated (Total) Acceptance Electrons

for the two 20 x 20 x 20 cm^3 E detectors

Sampex had 1.7 cm2sr

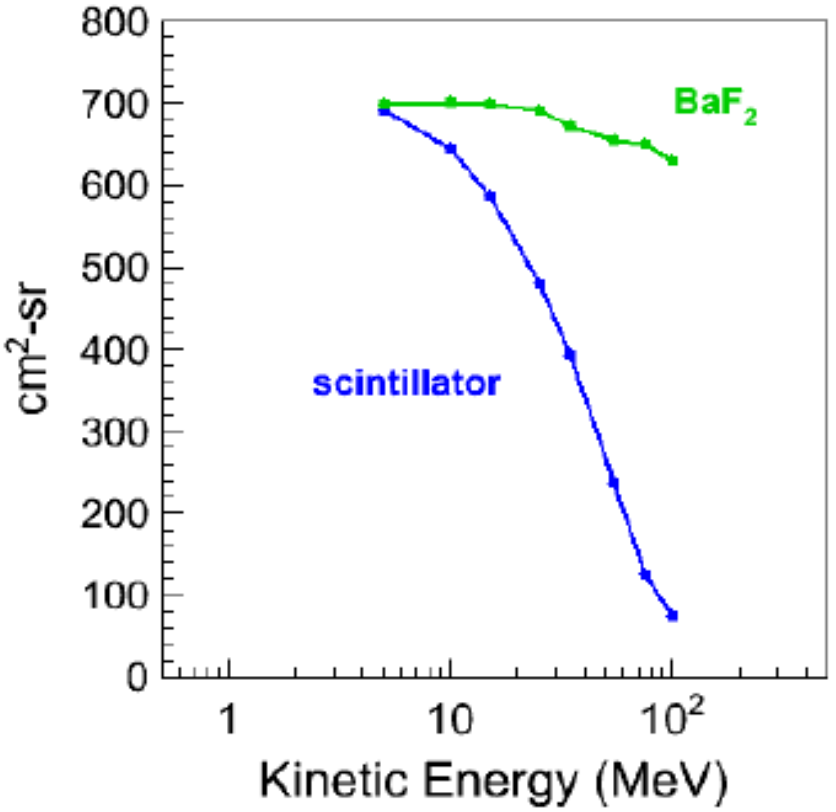

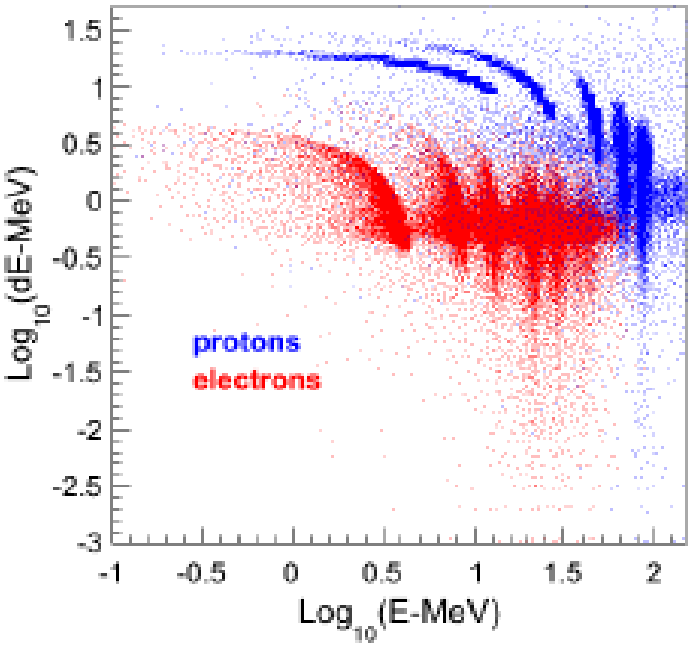

W.Burger

CSES :The High Energy Particle Detector

Flux Estimates for Background Determination

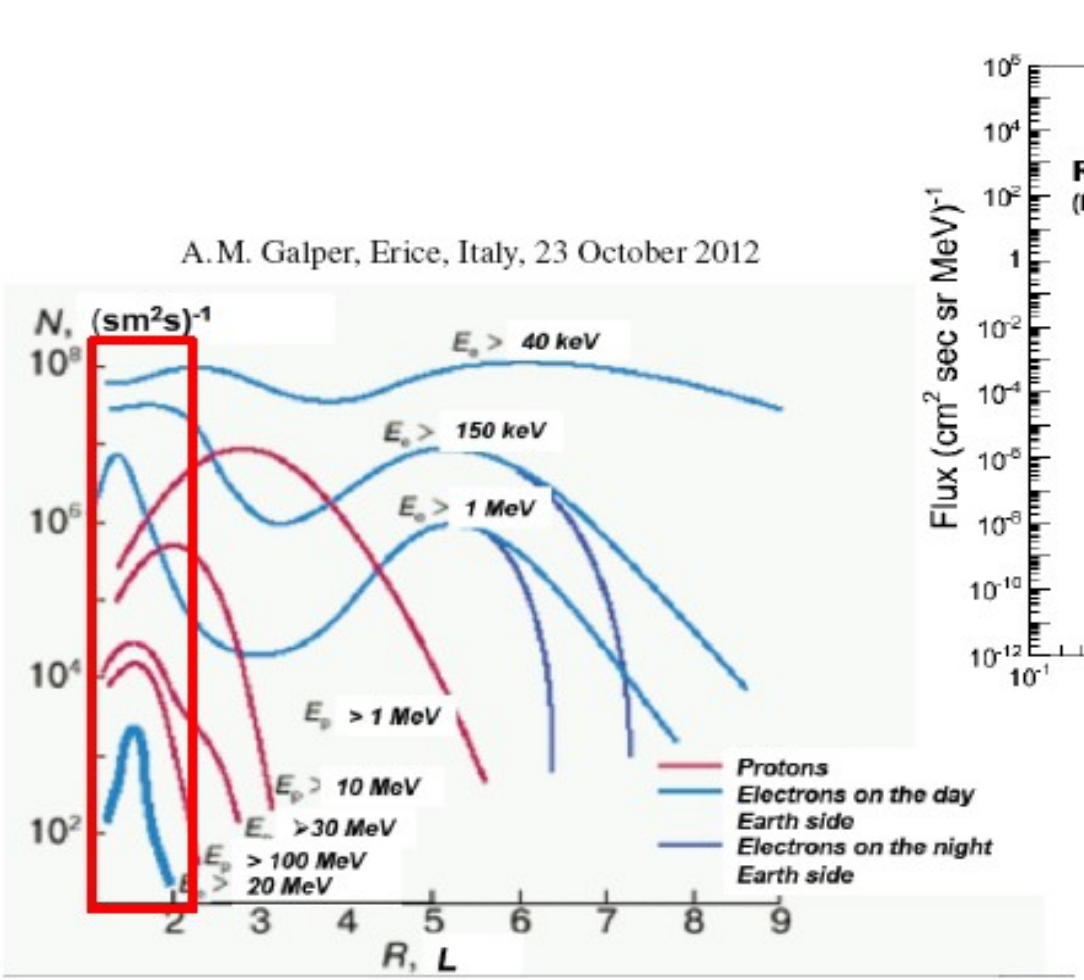

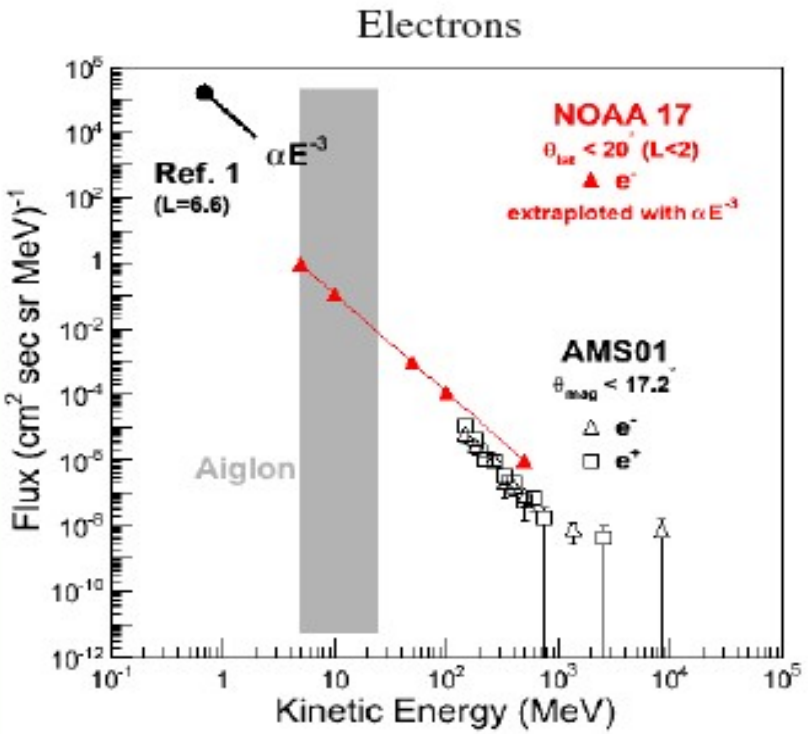

W.Burger

CSES :The High Energy Particle Detector

Current Status

The energy resolution performance of Aiglon-E (5-10 % between 5-35 MeV) is comparable to the version magnetic spectrometer.

The angular resolution is improved with the sacrifice of the TOF measure, but *a priori,* performace for proton/electron separation depends on β, common to the different measurement techniques.

The angular acceptance is very good. A reduction of the dimensions of the calormeter affects both the angular and energy acceptances.

The performance for protons has not be studied.

W.Burger